Journal of Computational Mathematics
Vol.31, No.2, 2013, 107–136.
http://www.global-sci.org/jcm
doi:10.4208/jcm.1210-m4094

A MULTI-DOMAIN SPECTRAL IPDG METHOD FOR HELMHOLTZ EQUATION WITH HIGH WAVE NUMBER*

Lunji Song
School of Mathematics and Statistics, Lanzhou University, Lanzhou 730000, China
Email: song@lzu.edu.cn
Jing Zhang
School of Mathematics and Statistics, Huazhong Normal University, Wuhan 430079, China
Email: zjccnu@gmail.com
Li-Lian Wang
Division of Mathematical Sciences, School of Physical and Mathematical Sciences, Nanyang Technological University, 637371, Singapore
Email: lilian@ntu.edu.sg

Abstract

This paper is concerned with a multi-domain spectral method, based on an interior penalty discontinuous Galerkin (IPDG) formulation, for the exterior Helmholtz problem truncated via an exact circular or spherical Dirichlet-to-Neumann (DtN) boundary condition. An effective iterative approach is proposed to localize the global DtN boundary condition, which facilitates the implementation of multi-domain methods, and the treatment for complex geometry of the scatterers. Under a discontinuous Galerkin formulation, the proposed method allows to use polynomial basis functions of different degree on different subdomains, and more importantly, explicit wave number dependence estimates of the spectral scheme can be derived, which is somehow implausible for a multi-domain continuous Galerkin formulation.

Mathematics subject classification: 65N35, 65E05, 65M70, 41A05, 41A10, 41A25.
Key words: Helmholtz equation, High wavenumber, Global DtN boundary condition, IPDG, Multli-domain spectral method.

1. Introduction

Time harmonic wave propagations appear in many applications, and a variety of situations requires to solve the Helmholtz equation exterior to a bounded obstacle (or scatterer):

$$\begin{cases} -\Delta u - k^2 u = f, & \text{in} \quad \Omega_e := \mathbb{R}^d \setminus B, \\ u = g, & \text{on} \quad \Gamma_B := \partial B, \\ \partial_r u - \mathrm{i}ku = o\big(r^{\frac{1-d}{2}}\big), & \text{as} \quad r \to \infty, \end{cases} \tag{1.1}$$

where $k>0$ is the wave number, $B \subset \mathbb{R}^d$, $d = 2, 3$ is a scatterer with Lipschitz boundary Γ_B, and the far-field boundary condition is known as the Sommerfeld radiation condition. On the surface of the obstacle B, the Dirichlet boundary condition corresponding to sound soft surface of B is imposed, while the Neumann or Robin boundary condition relative to sound hard or

* Received March 3, 2012 / Revised version received October 9, 2012 / Accepted October 25, 2012 / Published online March 14, 2013 /

impedance surface, respectively, may also be prescribed in practice. In fact, the method to be proposed in this paper works for these possible boundary conditions.

Apparent challenges in solving the exterior Helmholtz equation lie in (i) the domain is unbounded, (ii) the problem is indefinite, and (iii) the solution is highly oscillatory (when the wave number is large) and decays slowly. There is a vast literature devoted to its numerical solutions such as boundary element methods [9], infinite element methods [17], Dirichlet-to-Neumann (DtN) methods [23], perfectly matched layers (PML) [6], among others. In many of these approaches, it is essential to truncate the unbounded domain to a bounded domain by imposing an exact or approximate non-reflecting boundary condition at the outer boundary. Formally, the problem (1.1) reduces to

$$\begin{cases} -\Delta u - k^2 u = f, & \text{in} \quad \Omega := \Omega_R \setminus \bar{B}, \\ u = g, & \text{on} \quad \Gamma_B, \\ \partial_r u + Gu = 0, & \text{on} \quad \Gamma_R, \end{cases} \tag{1.2}$$

where Ω_R is an artificial domain that encloses the bounded scatterer B and contains the support of f, and the Robin boundary involving the operator G describes a typical transparent or non-reflecting boundary condition on the outer boundary Γ_R of Ω_R. For instance, G can be the Dirichlet-to-Neumann operator, which has a series expansion when Ω_R is a separable domain, e.g., disk, ball, ellipse and ellipsoid.

In the past two decades, there has been an intensive research on the finite element discretization of (1.2) in various situations (see, e.g., [3–5, 20–22] and the references therein). It is known that when the wave number k becomes large, the mesh size h should be adapted to k so as to resolve the waves. In two or higher dimensions, under the "rule of thumb" mesh constraints $kh \lesssim 1$, the pollution effect exits for all degrees of approximation and deteriorate the error estimates [20]. Thus, it is important to appreciate how the numerical errors depending on the wave numbers. Babuška et al. [20–22] conducted a rigorous analysis using the (discrete) Green's functions, and Douglas et al. [13] used a different argument due to Schatz [32]. However, these approaches may not be applicable to (1.2) with a slightly complicated setting of boundary conditions or scatterers. Recently, some methodology was developed in [11, 24] (also see [7, 19, 25, 34]) for the *a prior* estimates of the solution of (1.2) in a star-shaped domain Ω.

The spectral method, which is vitally free of dispersive errors, is well-suited for wave simulations. With a proper boundary perturbation technique (or the so-called transformed field expansion) [28], the Helmholtz equation (1.2) with exact DtN boundary condition can be reduced to a sequence of Helmholtz equations in a separable domain, e.g., an annulus and a spherical shell (cf. [14, 29, 30, 33]). Shen and Wang [35] provided a rigorous analysis of the spectral-Galerkin method with explicit dependence of the errors on the wave number for the Helmholtz equation in an annulus or spherical shell with exact DtN boundary condition. The analysis for full coupled spectral-Galerkin and boundary perturbation was conducted in [30]. Indeed, within the domain of applicability of the boundary perturbation method, this approach has proven to be fast and accurate. However, an element method is more desirable, when the scatterer is complex with a large deviation from a "simple" domain.

The purpose of this paper is to propose and analyze a multi-domain spectral interior penalty discontinuous Galerkin (in short, p-IPDG) method, for (1.2) with an exact DtN boundary condition. We advocate a DG formulation for two reasons:

(i) flexibility for general scatters and benefit of p-adaptivity (different orders of polynomials might be used for different elements) by using the discontinuous Galerkin formulation (see, e.g., [1, 2, 10, 31] and the references therein).

(ii) appreciation of the IPDG methods for indefinite Helmholtz problems with large wave number and global DtN boundary condition. Indeed, the available argument in [11, 24] does not work for the element method based on a continuous Galerkin formulation (cf. [15]), but it is plausible for the IPDG approach.

It is important to mention the recent work of Feng and Wu [15], where an interior penalty DG piecewise linear finite-element method was analyzed for (1.2) with $G = \mathrm{i}k$ (a first-order approximation of the Sommerfeld boundary condition). Our method distinguishes itself from the existing ones in several aspects. Firstly, to achieve high-order accuracy, we consider the exact non-reflecting boundary condition with G being the DtN map, and introduce an efficient iterative approach to treat this global boundary conditions to fully decouple the unknowns in an element method. Secondly, we find that the penalty along the normal direction is sufficient in our method, rather than additional penalty in the tangential direction in [15], which is more convenient for implementation and analysis. Moreover, we characterize the dependence of the penalty parameter on the edge length of each element (or subdomain), so the penalization could be very flexible and non-isotropic along each edge.

The rest of the paper is organized as follows. In Section 2, we propose an effective iterative approach to localize the global DtN boundary condition, and provide sufficient conditions for its convergence together with some numerical justifications. In Section 3, we formulate the p-IPDG scheme and analyze its stability. Then, we estimate the convergence of the iterative multi-domain spectral-IPDG scheme in Section 4. The final section is for some numerical results.

2. Localization of the DtN Map: An Iterative Approach

Consider the truncated Helmholtz equation (1.2) with $g = 0$, Ω_R being a disk or ball, and G being the exact DtN operator. More precisely, the problem of interest takes the form:

$$\begin{cases} -\Delta u - k^2 u = f, & \text{in } \Omega = \Omega_R \setminus \bar{B}, \\ u = 0, & \text{on } \Gamma_B, \\ \partial_r u + Tu = 0, & \text{on } \Gamma_R, \end{cases} \tag{2.1}$$

where T is the DtN map to be specified below, and we refer to Fig. 2.1 the underlying setup. We first review the expression of the DtN map, and then introduce an iterative approach to localize this global boundary condition.

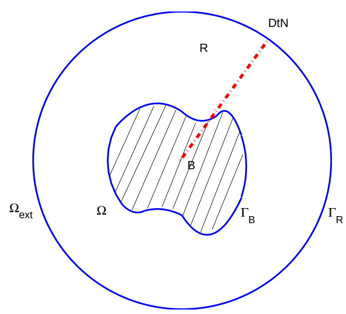

Fig. 2.1. Truncation via DtN.

2.1. Dirichlet-to-Neumann map

The exact circular or spherical DtN nonreflecting boundary condition can be obtained by solving the Helmholtz equation exterior to Ω with $f = 0$ and given Dirichlet data $u|_{\Gamma_R}$ (see, e.g., [27]). Recall that

- for $d = 2$,

$$Tu = -\frac{\partial u}{\partial r}\Big|_{r=R} = -\sum_{l=-\infty}^{\infty} k \frac{\partial_z H_l^{(1)}(kR)}{H_l^{(1)}(kR)} \hat{u}_l e^{\mathrm{i}l\theta}, \tag{2.2}$$

  where $\theta \in [0, 2\pi)$, $H_l^{(1)}$ is the Hankel function of the first kind of order l (cf. [26]), and $\{\hat{u}_l\}$ are the Fourier expansion coefficients of $u|_{r=R}$;

- for $d = 3$,

$$Tu = -\sum_{l=0}^{\infty} k \frac{\partial_z h_l^{(1)}(kR)}{h_l^{(1)}(kR)} \sum_{m=-l}^{l} \hat{u}_{lm} Y_l^m(\theta, \phi), \tag{2.3}$$

  where $h_l^{(1)}(z)$ is the spherical Hankel function of the first kind of order l, and $\{Y_l^m\}$ are the spherical harmonic function (cf. [26,27]), and $\{\hat{u}_{lm}\}$ are the spherical harmonic expansion coefficients of $u|_{r=R}$.

For notational convenience, we use $T_{m,\kappa}$ with $\kappa = kR$ to denote the DtN kernel:

$$T_{m,\kappa} = \frac{H_m^{(1)'}(\kappa)}{H_m^{(1)}(\kappa)}, \ \text{ if } \ d = 2; \quad T_{m,\kappa} = \frac{h_m^{(1)'}(\kappa)}{h_m^{(1)}(\kappa)}, \ \text{ if } \ d = 3. \tag{2.4}$$

We summarize some basic properties of $T_{m,\kappa}$ (cf. [27, 35]) to be used in the forthcoming analysis.

(i) For the 2-D kernel $T_{m,\kappa}$, we have $T_{m,\kappa} = T_{-m,\kappa}$, and

$$0 < \mathrm{Im}(T_{m,\kappa}) < 1, \quad -\frac{m}{\kappa} \le \mathrm{Re}(T_{m,\kappa}) \le -\frac{1}{2\kappa}, \quad m \ge 1, \tag{2.5}$$

$$\mathrm{Im}(T_{0,\kappa}) > 1, \quad \kappa > 0, \quad -\frac{1}{2\kappa} \le \mathrm{Re}(T_{0,\kappa}) < 0. \tag{2.6}$$

(ii) For the 3-D kernel $T_{m,\kappa}$, we have

$$-\frac{m+1}{\kappa} \le \mathrm{Re}(T_{m,\kappa}) \le -\frac{1}{\kappa}, \quad 0 < \mathrm{Im}(T_{m,\kappa}) \le 1, \quad m \ge 1, \tag{2.7}$$

$$\mathrm{Re}(T_{0,\kappa}) = -\frac{1}{\kappa}, \quad \mathrm{Im}(T_{0,\kappa}) = 1. \tag{2.8}$$

(iii) The monotonic properties hold for both 2-D and 3-D kernels: (a) for fixed $m \ge 1$, $\mathrm{Im}(T_{m,\kappa})$ is strictly increasing with respect to κ; and (b) for fixed $\kappa > 0$, we have $\mathrm{Im}(T_{m,\kappa}) > \mathrm{Im}(T_{m+1,\kappa}), m \ge 0$.

The Dirichlet-to-Neumann map given in the previous section is global in character, so the naive implementation of a local element method would result in the coupling of unknowns (at least of those elements along the outer boundary). The crux of the effective method is how to localize the DtN boundary condition without losing the accuracy.

2.2. The iterative scheme and its convergence

Hereafter, let D_k be a local operator, which only depends on the wave number k and the radius R. We propose the following iterative scheme to solve (2.1):

$$\begin{cases} -\Delta u^{n+1} - k^2 u^{n+1} = f, & \text{in } \Omega, \\ u^{n+1} = 0, & \text{on } \Gamma_B, \\ \partial_r u^{n+1} + kD_k u^{n+1} = (kD_k - T)u^n, & \text{on } \Gamma_R, \end{cases} \tag{2.9}$$

for $n \geq 0$ with given u^0. In contrast to (2.1), the Robin boundary condition in (2.9) at the outer boundary becomes local. Now, the important issue is how to choose D_k so that (i) (2.9) is well-posed, and (ii) the sequence $\{u^n\}$ converges fast to the solution u of (2.1).

With regard to the first issue, it suffices to require (cf. [12, 18]) that

$$\mathrm{Re}\big(D_k\big) \geq 0, \quad \mathrm{Im}\big(D_k\big) < 0, \quad \text{for } d = 2, 3, \tag{2.10}$$

to ensure the well-posedness of (2.9) as with the original problem (2.1).

Now, we turn to the second issue. Since the analysis for $d = 2, 3$ is very similar, we restrict our attention to the 2-D analysis for the sake of clarity.

We first introduce some notation. Let $L^2(\Omega)$ be the Hilbert space of complex-valued functions with inner product and norm, denoted by $(\cdot,\cdot)$ and $\|u\|_{L^2(\Omega)}$, respectively. In particular, $\langle\cdot,\cdot\rangle_{\partial\Omega}$ is the L^2-inner product on complex-valued $L^2(\partial\Omega)$ spaces. Then the Sobolev spaces $H^s(\Omega)$ $(s \geq 1)$ can be defined as usual with norms, and seminorms denoted by $\|\cdot\|_{H^s(\Omega)}$, and $|\cdot|_{s,\Omega}$, respectively. We also use the wave number dependent H^1-norm:

$$|||u|||_{1,\Omega} := \Big(|u|_{1,\Omega}^2 + k^2\|u\|_{L^2(\Omega)}^2\Big)^{1/2}. \tag{2.11}$$

The following assumptions and conventions are assumed in the analysis:

(a) the scatterer B is star-shaped, i.e., there exist $x_B \in B$ and a constant C_B such that

$$(x - x_B)\cdot \boldsymbol{n}_{\Gamma_B} \geq C_B \geq 0, \quad \forall\, x \in \Gamma_B, \tag{2.12}$$

where $\boldsymbol{n}_{\Gamma_B}$ is the unit vector outer normal to B.

(b) the wave number satisfies $k \geq k_0 > 0$.

(c) the radius R of the artificial disk or ball satisfies $R > R_0 > 0$, for some constant R_0.

For notational convenience, we denote

$$\delta_{m,kR} := D_k + T_{m,kR}, \quad \delta_{m,kR}^R := \mathrm{Re}(\delta_{m,kR}), \quad \delta_{m,kR}^I := \mathrm{Im}(\delta_{m,kR}), \tag{2.13}$$

where $T_{m,kR}$ is defined in (2.4).

Now, we are ready to present the main result on the convergence of the iterative scheme (2.9), which provides the sufficient conditions for the choice of D_k.

Theorem 2.1. *Let u and u^{n+1} be the solutions of* (2.1) *and* (2.9)*, respectively, and let $e^{n+1} := u - u^{n+1}$. Assuming that D_k satisfies* (2.10) *and the assumptions* (a)-(c) (*with $x_B = 0$ in* (2.12)) *hold, we have for $d = 2$,*

$$\begin{aligned} &|||e^{n+1}|||_{1,\Omega}^2 + \big(Rk^2\mathrm{Im}(D_k)^2 + k\mathrm{Re}(D_k)\big)\|e^{n+1}\|_{L^2(\Gamma_R)}^2 + R\|\nabla_T e^{n+1}\|_{L^2(\Gamma_R)}^2 + C_B\big\|\partial_\mu e^{n+1}\big\|_{L^2(\Gamma_B)}^2 \\ &\qquad \leq S_1(k)\big(Rk^2\mathrm{Im}(D_k)^2 + k\mathrm{Re}(D_k)\big)\|e^n\|_{L^2(\Gamma_R)}^2 + S_2(k)R\|\nabla_T e^n\|_{L^2(\Gamma_R)}^2, \end{aligned} \tag{2.14}$$

where

$$
\begin{aligned}
S_1(k) &= \frac{k^2 W(k)}{Rk^2 \mathrm{Im}(D_k)^2 + k\mathrm{Re}(D_k)} |\delta_{0,kR}|^2, \\
S_2(k) &= \frac{k^2 W(k)}{R} \max_{|m|\neq 0} \big\{ (|m|^{-1}\delta_{m,kR})^2 \big\},
\end{aligned}
\tag{2.15}
$$

with

$$
W(k) := \frac{3R}{2} + \frac{R(\mathrm{Re}(D_k)^2+1))}{\mathrm{Im}(D_k)^2} + \frac{(1-2kR\mathrm{Re}(D_k))^2}{2k^2R\mathrm{Im}(D_k)^2}. \tag{2.16}
$$

Therefore, by choosing D_k *such that*

$$
S_i(k) < 1, \quad i = 1, 2, \tag{2.17}
$$

we have the convergence

$$
|||u - u^n|||_{1,\Omega} \to 0, \quad \text{as } n \to \infty. \tag{2.18}
$$

Proof. We find from (2.1) and (2.9) that e^{n+1} satisfies

$$
\begin{cases}
-\Delta e^{n+1} - k^2 e^{n+1} = 0, & \text{in } \Omega, \\
e^{n+1} = 0, & \text{on } \Gamma_B, \\
\partial_r e^{n+1} + kD_k e^{n+1} = \delta_k e^n, & \text{on } \Gamma_R,
\end{cases}
\tag{2.19}
$$

where $\delta_k := kD_k - T$ (cf. (2.9)) and $e^0 = u - u^0$.

Suppose that $G \subset \mathbb{R}^d$ is a bounded Lipschitz domain with a boundary ∂G and that $v \in H^2(G)$. Then for every $k \geq 0$, set $g := \Delta v + k^2 v$ and let μ be the unit normal vector pointing out of G. Let $\nabla_T \bar{v}$ be the tangential derivative on $\partial\Omega$. Similar to Lemma 2.3 in [7], we have

$$
\int_G (|\nabla v|^2 - k^2|v|^2 + g\bar{v}) dx = \int_{\partial G} \bar{v} \frac{\partial v}{\partial \mu} ds,
$$

and

$$
\begin{aligned}
&\int_G ((2-d)|\nabla v|^2 + dk^2|v|^2 + 2\mathrm{Re}(gx\cdot\nabla\bar{v}))dx \\
&= \int_{\partial G} \Big(x\cdot\mu \Big(k^2|v|^2 + \Big|\frac{\partial v}{\partial\mu}\Big|^2 - |\nabla_T v|^2 \Big) + 2\mathrm{Re}\Big(x\cdot\nabla_T\bar{v}\frac{\partial v}{\partial \mu}\Big)\Big) ds.
\end{aligned}
$$

Applying the above identities to (2.19), we find that

$$
\int_\Omega \big(|\nabla e^{n+1}|^2 - k^2|e^{n+1}|^2 \big)\, dx = \int_{\partial\Omega} \frac{\partial e^{n+1}}{\partial\mu} \overline{e^{n+1}} ds, \tag{2.20}
$$

and

$$
\begin{aligned}
&\int_\Omega \big((2-d)|\nabla e^{n+1}|^2 + dk^2|e^{n+1}|^2 \big)\, dx \\
&= \int_{\partial\Omega} \Big\{ x\cdot\mu \Big(k^2|e^{n+1}|^2 + \Big|\frac{\partial e^{n+1}}{\partial\mu}\Big|^2 - |\nabla_T e^{n+1}|^2 \Big) + 2\mathrm{Re}\Big(x\cdot\nabla_T\overline{e^{n+1}}\frac{\partial e^{n+1}}{\partial\mu}\Big)\Big\} ds.
\end{aligned}
\tag{2.21}
$$

Using the homogeneous Dirichlet boundary condition on Γ_B, and adding $(d-1)$ times the real part of (2.20) to (2.21), we obtain

$$\begin{aligned}\int_\Omega \big(|\nabla e^{n+1}|^2 + k^2|e^{n+1}|^2\big)\,dx &= -\int_{\Gamma_B} x\cdot \boldsymbol{n}_{\Gamma_B}\Big|\frac{\partial e^{n+1}}{\partial \boldsymbol{n}_{\Gamma_B}}\Big|^2 ds \\ &+ \int_{\Gamma_R}\Big\{x\cdot\mu\Big(k^2|e^{n+1}|^2 + \Big|\frac{\partial e^{n+1}}{\partial\mu}\Big|^2 - |\nabla_T e^{n+1}|^2\Big) + \mathrm{Re}\Big((d-1)\frac{\partial e^{n+1}}{\partial\mu}\overline{e^{n+1}}\Big)\Big\}ds,\end{aligned} \tag{2.22}$$

where we have used the facts

$$\nabla_T e^{n+1} = 0, \quad \text{on } \Gamma_B; \quad x\cdot\nabla_T\overline{e^{n+1}} = 0, \quad \text{on } \Gamma_R. \tag{2.23}$$

Since B is a star-shaped scatter (cf. (2.12) with $x_B = 0$), we obtain from (2.22) that

$$\begin{aligned}&\int_\Omega (\nabla e^{n+1}|^2 + k^2|e^{n+1}|^2)dx + C_B\Big\|\frac{\partial e^{n+1}}{\partial\mu}\Big\|^2_{L^2(\Gamma_B)} + R\|\nabla_T e^{n+1}\|^2_{L^2(\Gamma_R)} \\ \le &\int_{\Gamma_R} R\Big(k^2|e^{n+1}|^2 + \Big|\frac{\partial e^{n+1}}{\partial\mu}\Big|^2\Big) + \mathrm{Re}\Big((d-1)\overline{e^{n+1}}\frac{\partial e^{n+1}}{\partial\mu}\Big)ds.\end{aligned} \tag{2.24}$$

Thus, it is enough to bound the term on the right hand side of (2.24). Notice that by the Robin boundary condition, the right hand side of (2.24) becomes

$$\begin{aligned}&\text{RHS of (2.24)} \\ =&\int_{\Gamma_R} R\big(k^2|e^{n+1}|^2 + |\delta_k e^n - kD_k e^{n+1}|^2\big) + (d-1)\mathrm{Re}\Big(\big(\delta_k e^n - kD_k e^{n+1}\big)\overline{e^{n+1}}\Big)ds \\ =&\int_{\Gamma_R}\Big(R\big(k^2|e^{n+1}|^2 + |\delta_k e^n - kD_k e^{n+1}|^2\big) \\ &\quad + (d-1)\mathrm{Re}\big(\delta_k e^n\overline{e^{n+1}}\big) - (d-1)k\mathrm{Re}(D_k)|e^{n+1}|^2\Big)ds.\end{aligned} \tag{2.25}$$

Multiplying the first equation of (2.19) by $\overline{e^{n+1}}$, integrating the resulted equation over Ω, and using the Green's formula and the boundary conditions, we find that the imaginary part of the resulted equation is

$$\mathrm{Im}\Big(\int_{\Gamma_R}\big(\delta_k e^n - kD_k e^{n+1}\big)\overline{e^{n+1}}ds\Big) = 0, \tag{2.26}$$

which implies

$$k|\mathrm{Im}(D_k)|\|e^{n+1}\|^2_{L^2(\Gamma_R)} = \big|\mathrm{Im}\langle\delta_k e^n, e^{n+1}\rangle_{\Gamma_R}\big|.$$

Thus, by the Cauchy-Schwarz inequality,

$$\|e^{n+1}\|^2_{L^2(\Gamma_R)} \le \frac{1}{k^2|\mathrm{Im}(D_k)|^2}\|\delta_k e^n\|^2_{L^2(\Gamma_R)}. \tag{2.27}$$

Notice that

$$\begin{aligned}\int_{\Gamma_R} R|\delta_k e^n - kD_k e^{n+1}|^2 ds = &\int_{\Gamma_R}\Big\{R|\delta_k e^n|^2 + Rk^2|D_k|^2|e^{n+1}|^2 \\ &- 2kR\big(\mathrm{Re}(D_k e^{n+1})\mathrm{Re}(\delta_k e^n) + \mathrm{Im}(D_k e^{n+1})\mathrm{Im}(\delta_k e^n)\big)\Big\}ds.\end{aligned} \tag{2.28}$$

By splitting the second term in the above identity into $Rk^2\mathrm{Im}(D_k)^2|e^{n+1}|^2$ and $Rk^2\mathrm{Re}(D_k)^2$ $|e^{n+1}|^2$, and using (2.26), we derive

$$\begin{aligned}
&\int_{\Gamma_R}\Big\{Rk^2\mathrm{Im}(D_k)^2|e^{n+1}|^2-2kR\Big(\mathrm{Re}(D_ke^{n+1})\mathrm{Re}(\delta_ke^n)+\mathrm{Im}(D_ke^{n+1})\mathrm{Im}(\delta_ke^n)\Big)\Big\}ds\\
=&\int_{\Gamma_R}\Big\{Rk\mathrm{Im}(D_k)\Big(-\mathrm{Im}(e^{n+1})\mathrm{Re}(\delta_ke^n)+\mathrm{Re}(e^{n+1})\mathrm{Im}(\delta_ke^n)\Big)\\
&+2kR\Big(-\mathrm{Re}(D_k)\mathrm{Re}(e^{n+1})\mathrm{Re}(\delta_ke^n)+\mathrm{Im}(D_k)\mathrm{Im}(e^{n+1})\mathrm{Re}(\delta_ke^n)\\
&-\mathrm{Im}(D_k)\mathrm{Re}(e^{n+1})\mathrm{Im}(\delta_ke^n)-\mathrm{Re}(D_k)\mathrm{Im}(e^{n+1})\mathrm{Im}(\delta_ke^n)\Big)\Big\}ds\\
=&\int_{\Gamma_R}\Big\{-Rk^2\mathrm{Im}(D_k)^2|e^{n+1}|^2-2kR\mathrm{Re}(D_k)\mathrm{Re}(e^{n+1}\overline{\delta_ke^n})\Big\}ds, \qquad (2.29)
\end{aligned}$$

where we have used the facts due to (2.26) as follows

$$\begin{aligned}
&\int_{\Gamma_R}Rk^2\mathrm{Im}(D_k)^2|e^{n+1}|^2ds\\
=&\int_{\Gamma_R}\big\{-Rk\mathrm{Im}(D_k)\mathrm{Im}(e^{n+1})\mathrm{Re}(\delta_ke^n)+Rk\mathrm{Im}(D_k)\mathrm{Re}(e^{n+1})\mathrm{Im}(\delta_ke^n)\big\}ds.
\end{aligned}$$

Inserting (2.29) into (2.28) leads to

$$\begin{aligned}
&\int_{\Gamma_R}R|\delta_ke^n-kD_ke^{n+1}|^2ds \qquad (2.30)\\
=&\int_{\Gamma_R}\Big\{R|\delta_ke^n|^2+Rk^2\mathrm{Re}(D_k)^2|e^{n+1}|^2-Rk^2\mathrm{Im}(D_k)^2|e^{n+1}|^2-2kR\mathrm{Re}(D_k)\mathrm{Re}(e^{n+1}\overline{\delta_ke^n})\Big\}ds.
\end{aligned}$$

So it follows from (2.25) and (2.30) that

$$\begin{aligned}
&\text{RHS of (2.24)}\\
=&\int_{\Gamma_R}R|\delta_ke^n|^2+\Big(Rk^2(\mathrm{Re}(D_k)^2+1)-(d-1)k\mathrm{Re}(D_k)-Rk^2\mathrm{Im}(D_k)^2\Big)|e^{n+1}|^2\\
&+(d-1)\mathrm{Re}(\delta_ke^n\overline{e^{n+1}})-2kR\mathrm{Re}(D_k)\mathrm{Re}(e^{n+1}\overline{\delta_ke^n})ds. \qquad (2.31)
\end{aligned}$$

For the last two terms on the right hand side of (2.31), noting that $\mathrm{Re}(\delta_ke^n\overline{e^{n+1}})=\mathrm{Re}(e^{n+1}\overline{\delta_ke^n})$, we derive from the Cauchy-Schwarz inequality that

$$\begin{aligned}
&\int_{\Gamma_R}(d-1)\mathrm{Re}(\delta_ke^n\overline{e^{n+1}})-2kR\mathrm{Re}(D_k)\mathrm{Re}(e^{n+1}\overline{\delta_ke^n})ds\\
=&(d-1-2kR\mathrm{Re}(D_k))\int_{\Gamma_R}\mathrm{Re}(\delta_ke^n\overline{e^{n+1}})ds\\
\le&\frac{R}{2}\int_{\Gamma_R}|\delta_ke^n|^2ds+\frac{(d-1-2kR\mathrm{Re}(D_k))^2}{2R}\int_{\Gamma_R}|e^{n+1}|^2ds.
\end{aligned}$$

Then a combination of (2.24), (2.27), and (2.31) leads to

$$\begin{aligned}
&|||e^{n+1}|||^2_{1,\Omega}+C_B\Big\|\frac{\partial e^{n+1}}{\partial\mu}\Big\|^2_{L^2(\Gamma_B)}+R\|\nabla_Te^{n+1}\|^2_{L^2(\Gamma_R)}\\
&+\Big(Rk^2\mathrm{Im}(D_k)^2+(d-1)k\mathrm{Re}(D_k)\Big)\|e^{n+1}\|^2_{L^2(\Gamma_R)}\le W(k)\|\delta_ke^n\|^2_{L^2(\Gamma_R)}, \qquad (2.32)
\end{aligned}$$

where $W(k)$ is defined in (2.16).

It remains to bound $\|\delta_k e^n\|_{L^2(\Gamma_R)}$. Recall that $\delta_k e^n = (kD_k - T)e^n$, and by (2.2) and (2.4),

$$(\delta_k e^n)(r,\theta) = \sum_{|m|=0}^{\infty} k(D_k + T_{m,kR})\hat{e}_m^n(r)e^{\mathrm{i}m\theta}, \quad \theta \in [0, 2\pi], \tag{2.33}$$

where $\{\hat{e}_m^n\}$ are the Fourier coefficients. Thus, using the notation in (2.13), we have from the Parseval's identity that

$$\begin{aligned}\int_{\Gamma_R} |\delta_k e^n|^2 ds &= 2\pi R k^2 \sum_{|m|=0}^{\infty} (\delta_{m,kR}^R)^2 \big|\hat{e}_m^n(R)\big|^2 + 2\pi R k^2 \sum_{|m|=0}^{\infty} (\delta_{m,kR}^I)^2 \big|\hat{e}_m^n(R)\big|^2 \\ &\leq 2\pi R k^2 |\delta_{0,kR}|^2 \big|\hat{e}_0^n(R)\big|^2 + 2\pi R k^2 \max_{|m|\neq 0} \big\{(|m|^{-1}\delta_{m,kR}^R)^2\big\} \sum_{|m|\neq 0}^{\infty} m^2 \big|\hat{e}_m^n(R)\big|^2 \\ &\quad + 2\pi R k^2 \max_{|m|\neq 0} \big\{(|m|^{-1}\delta_{m,kR}^I)^2\big\} \sum_{|m|\neq 0}^{\infty} m^2 \big|\hat{e}_m^n(R)\big|^2 \\ &\leq k^2 |\delta_{0,kR}|^2 \|e^n\|^2_{L^2(\Gamma_R)} + k^2 \max_{|m|\neq 0} \big\{(|m|^{-1}\delta_{m,kR})^2\big\} \|\nabla_T e^n\|^2_{L^2(\Gamma_R)}. \end{aligned} \tag{2.34}$$

Therefore, the desired estimate (2.14) follows from (2.32) and (2.34).

Finally, by choosing a suitable D_k satisfying (2.17), we get

$$\|\nabla_T e^n\|_{L^2(\Gamma_R)} \to 0, \quad \|e^n\|_{L^2(\Gamma_R)} \to 0, \quad \big\|\partial_\mu e^{n+1}\big\|_{L^2(\Gamma_B)} \to 0, \quad \text{as } n \to \infty.$$

By (2.14), we also have $|||e^{n+1}|||_{1,\Omega} \to 0$ $(n \to \infty)$. □

Remark 2.1. The main argument is essentially the same as in [11, 24, 25]. Though we just stated the convergence result for $d = 2$, the analysis for $d = 3$ is very similar by using spherical harmonics in (2.33) and (2.34). Indeed, the situation is reminiscent to the proof of [35, Lemma 3.1], where the case with $d = 3$ is slightly easier to handle than the case $d = 2$.

For a better appreciation of the sufficient conditions on D_k in Theorem 2.1, we provide some sample selections of D_k .

2.2.1. Case I

Choose $D_k = -T_{0,kR}$, defined by (2.4) with $d = 2$. We find from (2.6) that D_k meets (2.10). Moreover, we have $\delta_{0,kR} = 0$, and $S_1(k) = 0 < 1$.

To justify this claim, using the facts $\mathrm{Im}(T_{0,kR}) > 1$ and $-\frac{1}{2kR} \leq \mathrm{Re}(T_{0,kR}) < 0$, leads to

$$W(k) \leq \frac{5}{2}R + \frac{9}{4k^2 R}. \tag{2.35}$$

Note that

$$\mathrm{Im}(T_{0,\kappa}) = \frac{2}{\pi\kappa}\frac{1}{J_0^2(\kappa) + Y_0^2(\kappa)} = \frac{2}{\pi\kappa |H_0^{(1)}(\kappa)|^2}. \tag{2.36}$$

Since the term $\kappa(J_0^2(\kappa) + Y_0^2(\kappa))$ is an increasing function of κ (cf. [36, Page 446]), then we have

$$1 < \mathrm{Im}(T_{0,\kappa}) \leq \frac{2}{\pi k_0 R_0 |H_0^{(1)}(k_0 R_0)|^2}, \tag{2.37}$$

where we used the assumption $kR \ge k_0R_0$.

We estimate the bound of $\max(|m|^{-1}\delta^I_{m,kR})^2$ for $|m| \neq 0$. We will use the facts that $0 < \mathrm{Im}(T_{m,kR}) < 1$ ($m \neq 0$) and an accurate approximation for $\mathrm{Im}(T_{m,kR})$ is (cf. [35, Page 1962])

$$E_{m,\kappa} := \begin{cases} \sqrt{1-\frac{m^2}{\kappa^2}}, & \text{if} \quad \kappa > m \ge 1, \\ c_0 m^{-\frac{1}{3}}, & \text{if} \quad \kappa = m, \end{cases} \tag{2.38}$$

where $c_0 \approx 0.7954$.

For $\kappa > m \ge 1$, by (2.37) and (2.38), we get

$$\begin{aligned} (m^{-1}\delta^I_{m,kR})^2 &\le \Big(m^{-1}\Big(\frac{2}{\pi k_0R_0|H_0^{(1)}(k_0R_0)|^2} - \sqrt{1-\frac{m^2}{\kappa^2}}\Big)\Big)^2 \\ &\le \Big(m^{-1}\Big(\frac{2}{\pi k_0R_0|H_0^{(1)}(k_0R_0)|^2} - 1 + \frac{m^2}{\kappa^2}\Big)\Big)^2 \\ &= \Big(m^{-1}\Big(c^* + \frac{m^2}{\kappa^2}\Big)\Big)^2 \le \frac{4c^*}{\kappa^2}, \end{aligned}$$

where

$$c^* = \frac{2}{\pi k_0R_0|H_0^{(1)}(k_0R_0)|^2} - 1.$$

For $\kappa \le m$, we derive

$$(m^{-1}\delta^I_{m,kR})^2 < (m^{-1}\mathrm{Im}(T_{0,\kappa}))^2 \le \Big(m^{-1}\Big(\frac{2}{\pi k_0R_0|H_0^{(1)}(k_0R_0)|^2}\Big)\Big)^2 \le \frac{(c^*+1)^2}{\kappa^2}.$$

Consequently, we have

$$\max_{|m|\neq 0}(|m|^{-1}\delta^I_{m,kR})^2 \le \frac{(c^*+1)^2}{k^2R^2}. \tag{2.39}$$

For $|m| \neq 0$, by (2.5)-(2.6), we arrive at

$$(|m|^{-1}\delta^R_{m,kR})^2 < \Big(|m|^{-1}\frac{|m|}{kR}\Big)^2 = \frac{1}{k^2R^2},$$

Then we estimate the bound of $S_2(k)$

$$S_2(k) \le \frac{k^2}{R}\Big(\frac{5}{2}R + \frac{9}{4k^2R}\Big)\frac{(c^*+1)^2+1}{k^2R^2} \le \Big(\frac{5}{2} + \frac{9}{4k_0^2R_0^2}\Big)\frac{(c^*+1)^2+1}{R^2}.$$

Consequently, if

$$R > \max\Big\{\Big(\Big(\frac{5}{2} + \frac{9}{4k_0^2R_0^2}\Big)\big((c^*+1)^2+1\big)\Big)^{\frac{1}{2}}, R_0\Big\},$$

then $S_2(k) < 1$.

Here, we provide some reference values of c^* :

$$(k_0R_0, c^*) = (0.1, 0.90098), (0.2, 0.48124), (0.3, 0.32015), (0.5, 0.18076), (1, 0.07298). \tag{2.40}$$

Note that c^* decreases as k_0R_0 increases.

2.2.2. Case II

Choose D_k such that $\mathrm{Re}(D_k) = 0$ and $\mathrm{Im}(D_k) = -1$, i.e., the first-order approximation of T. It follows from (2.37) that

$$|\delta_{0,kR}|^2 = |\mathrm{Re}(T_{0,k})|^2 + |\mathrm{Im}(T_{0,k}) - 1|^2 \le \frac{1}{4k^2R^2} + c^{*2}.$$

We have $W(k) = \frac{5}{2}R + \frac{1}{2k^2R}$, and

$$S_1(k) = \frac{W(k)|\delta_{0,kR}|^2}{R} \le \Big(\frac{5}{2} + \frac{1}{2k^2R^2}\Big)\Big(\frac{1}{4k^2R^2} + c^{*2}\Big) \le \Big(\frac{5}{2} + \frac{1}{2k^2R^2}\Big)\Big(\frac{1}{4k^2R^2} + c^{*2}\Big).$$

By direct computation, we see that $S_1(k) < 1$ holds if the condition

$$kR > \max\left\{\left(\sqrt{2 + \left(5 - 4c^{*2}\right)^2} + 5 + 4c^{*2}\right)\Big/ 2\left(8 - 20c^{*2}\right),\ k_0R_0\right\} \tag{2.41}$$

is satisfied with $c^* < 0.63246$ (e.g., $k_0R_0 \ge 0.2$, inferred from (2.40)). Therefore, $S_1(k) < 1$ if (2.41) holds.

For $m \ne 0$, we have

$$(|m|^{-1}\delta^R_{m,kR})^2 \le \Big(|m|^{-1}\frac{|m|}{kR}\Big)^2 = \frac{1}{k^2R^2}, \tag{2.42a}$$

$$(|m|^{-1}\delta^I_{m,kR})^2 = |m|^{-2}\big(1 - \mathrm{Im}(T_{m,kR})\big)^2. \tag{2.42b}$$

We estimate the bound of $\max(|m|^{-1}\delta^I_{m,kR})^2$. For $\kappa > m \ge 1$, by (2.38), we get

$$\big(m^{-1}(1 - \mathrm{Im}(T_{m,kR}))\big)^2 \le \Big(m^{-1}\Big(1 - \sqrt{1 - \frac{m^2}{\kappa^2}}\Big)\Big)^2 \le \Big(m^{-1}\Big(1 - 1 + \frac{m^2}{\kappa^2}\Big)\Big)^2 < \frac{1}{\kappa^2}.$$

For $\kappa \le m$, it holds that

$$\Big(m^{-1}(1 - \mathrm{Im}(T_{m,kR}))\Big)^2 \le m^{-2} < \frac{1}{\kappa^2}.$$

Consequently, we have

$$\max_{|m|\ne 0}(|m|^{-1}\delta^I_{m,kR})^2 < \frac{1}{k^2R^2}. \tag{2.43}$$

Then

$$S_2(k) \le \frac{k^2}{R}\Big(\frac{5}{2}R + \frac{1}{2k^2R}\Big)\frac{2}{k^2R^2} < \frac{1}{R^2}\Big(5 + \frac{1}{k_0^2R_0^2}\Big).$$

Therefore, if $R > \max\left\{\left(5 + \frac{1}{k_0^2R_0^2}\right)^{1/2}, R_0\right\}$, then $S_2(k) < 1$.

2.2.3. Case III

Choose D_k such that $\mathrm{Re}(D_k) = 0$ and $\mathrm{Im}(D_k) = -\mathrm{Im}(T_{0,kR})$. Similarly, we have

$$|\delta_{0,kR}|^2 = |\mathrm{Re}(T_{0,kR})|^2 \le \frac{1}{4k^2R^2},$$

$$W(k) = \frac{3}{2}R + \frac{R}{(\mathrm{Im}(T_{0,kR}))^2} + \frac{1}{2k^2R(\mathrm{Im}(T_{0,kR}))^2} < \frac{5}{2}R + \frac{1}{2k^2R}.$$

This leads to

$$S_1(k) \le \Big(\frac{5}{2} + \frac{1}{2k^2R^2}\Big)\frac{1}{4k^2R^2}.$$

Hence, as $k^2R^2 > 1$, then $S_1(k) < 1$.

For $m \ne 0$, it follows from (2.39) and (2.42) that

$$(|m|^{-1}\delta^R_{m,kR})^2 < \Big(|m|^{-1}\frac{|m|}{kR}\Big)^2 = \frac{1}{k^2R^2}, \quad (|m|^{-1}\delta^I_{m,kR})^2 \le \frac{(c^*+1)^2}{k^2R^2},$$

so we have

$$S_2(k) \le \frac{k^2}{R}\Big(\frac{5}{2}R + \frac{1}{2k^2R}\Big)\frac{(c^*+1)^2+1}{k^2R^2} = \Big(\frac{5}{2} + \frac{1}{2k_0^2R_0^2}\Big)\frac{(c^*+1)^2+1}{R^2}.$$

Finally, if

$$R > \max\Big\{\Big(\Big(\frac{5}{2} + \frac{1}{2k_0^2R_0^2}\Big)\big((c^*+1)^2+1\big)\Big)^{\frac{1}{2}}, R_0\Big\},$$

then $S_2(k) < 1$.

2.3. Numerical results

We feel compelled to provide some numerical results to illustrate the convergence of the proposed iterative scheme. To mimic the continuous setting, we discretize (2.9) with $d = 2$ and with the scatterer B being a disk, by a very accurate spectral solver in [35]. More specifically, we consider the following problem:

$$\begin{cases} -\Delta u^{n+1} - k^2 u^{n+1} = 0, \quad \text{in } \Omega := \big\{(x,y) \,:\, a^2 < x^2+y^2 < R^2\big\}, \\ u^{n+1}|_{r=a} = g, \\ (\partial_r + kD_k)u^{n+1}|_{r=R} = (kD_k - T)u^n|_{r=R}, \end{cases} \tag{2.44}$$

where $R > a > 0$ and g, u^0 are given.

Under the polar coordinates (r,θ), we expand the data and solution in Fourier series as

$$\big\{u^{n+1}(r,\theta), g(\theta)\big\} = \sum_{|m|=0}^{\infty} \big\{\hat u_m^{n+1}(r), \hat g_m\big\} e^{\mathrm{i}m\theta}.$$

Notice that T is given by (2.2). Then, the problem (2.44) reduces to a sequence of 1-D equations:

$$\begin{cases} -\dfrac{1}{r}\dfrac{d}{dr}\Big(r\dfrac{d}{dr}\hat u_m^{n+1}\Big) + m^2\dfrac{\hat u_m^{n+1}}{r^2} - k^2\hat u_m^{n+1} = 0, \quad r \in (a,R), \ \ |m| \ge 0, \\ \hat u_m^{n+1}(a) = \hat g_m, \\ \Big(\dfrac{d}{dr} + kD_k\Big)\hat u_m^{n+1}(R) = k(D_k + T_{m,kR})\hat u_m^n(R). \end{cases} \tag{2.45}$$

Thus, at each iteration, we use the spectral-Galerkin solver (cf. [35]) to update u^{n+1} from u^n.

Using the method of separation of variables, we find that (2.1) admits the solution:

$$u(r,\theta) = \sum_{|m|=0}^{\infty} \frac{H_m^{(1)}(kr)}{H_m^{(1)}(ka)}\hat g_m e^{\mathrm{i}m\theta}, \quad r \ge a, \ \ \theta \in [0,2\pi], \tag{2.46}$$

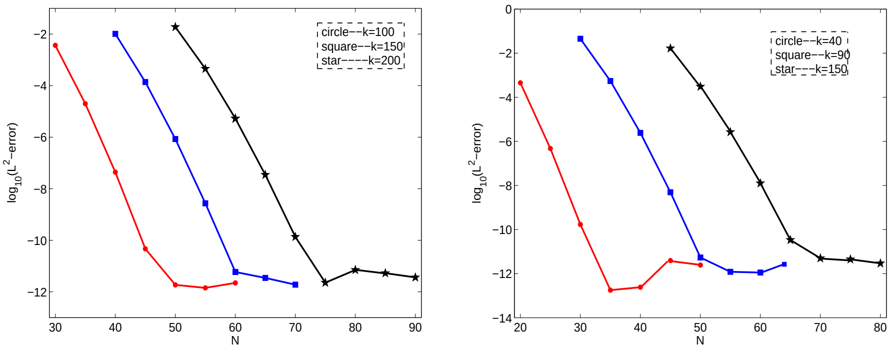

Fig. 2.2. Convergence of of the iterative scheme (2.44): L^2-errors against N. Left: Example 1 with $k = 100, 150, 200$. Right: Example 2 with $k = 40, 90, 140$.

which implies

$$\hat{u}_m(r) = \frac{H_m^{(1)}(kr)}{H_m^{(1)}(ka)} \hat{g}_m, \quad a < r < R,$$

satisfies the reduced one-dimensional problem.

In the following computations, we measure the errors: $E_N^n = \max_{|m|\le 50} \|\hat{u}_m^n - \hat{u}_{m,N}^n\|_\infty$, where $\hat{u}_{m,N}^n$ is the numerical solution obtained by the spectral-Galerkin scheme in [35] (with $N+1$ modes). We truncate up to $|m| \le 50$ in θ direction, so that the truncation error is negligible. We take $g(\theta) = \exp(\sin(\theta))$, and test two examples with the following setup:

- *Example* 1. Take $a = 1.4, R = 3, \mathrm{Re}(D_k) = 0$ and $\mathrm{Im}(D_k) = -\mathrm{Im}(T_{0,kR})$.
- *Example* 2. Take $a = 2.5, R = 4$ and $D_k = -T_{0,kR}$.

In Table 2.1 (resp. 2.2), we tabulate E_N^n and the number of iterations for various choices of k and N for Example 1 (resp. Example 2). The iteration is terminated when $\max_{|m|\le 50} \|\hat{u}_{m,N}^{n+1} - \hat{u}_{m,N}^n\|_\infty \le 10^{-12}$. We observe a fast convergence of the iterative scheme and spectral accuracy as N increases.

Table 2.1: Convergence of the iterative scheme (2.44) for Example 1.

$k=100$			$k=150$			$k=200$		
N	n	E_N^n	N	n	E_N^n	N	n	E_N^n
20	14	$3.63e-02$	40	17	$1.01e-02$	50	18	$1.88e-02$
30	15	$4.37e-08$	50	16	$8.48e-07$	60	12	$6.25e-06$
50	14	$1.87e-12$	60	14	$3.48e-12$	90	13	$3.51e-12$

Table 2.2: Convergence of the iterative scheme (2.44) for Example 2.

$k=40$			$k=90$			$k=140$		
N	n	E_N^n	N	n	E_N^n	N	n	E_N^n
20	20	$3.86e-04$	30	16	$4.30e-02$	45	17	$1.76e-02$
30	21	$1.69e-10$	40	20	$2.55e-06$	55	18	$2.64e-06$
50	17	$1.71e-12$	60	24	$8.67e-13$	70	14	$4.40e-12$

In Fig. 2.2, we plot the $\log_{10}$ of L^2-errors versus N for a wide range of k, and the stopping criterion is the same as before. We visualize a spectral accuracy even for large wave numbers. Indeed, these results verify the effectiveness of the localization technique.

3. The Multi-domain Spectral IPDG Method

In this section, we describe the multi-domain spectral interior penalty discontinuous Galerkin method for solving (2.9) with a general scatterer.

3.1. Notation and setup

We start with introducing the conventional notation and setup (see, e.g., [8,15,31]) for the discontinuous Galerkin method.

- Define the broken Sobolev space

$$\mathcal{S}^q := \prod_{k\in\mathcal{Q}_h} H^{q+1}(K), \quad q\geq 1, \tag{3.1}$$

  where $\mathcal{Q}_h$ is a partition of the computational domain Ω, and h is the discretization parameter for the mesh. In this context, each element $K\in\mathcal{Q}_h$ is a quadrilateral. For each edge/face e of an element $K\in\mathcal{Q}_h$, we denote $|e|:=\mathrm{diam}(e)$ and $h_K:=\mathrm{diam}(K)$. It is clear that

$$|e|\leq h_K. \tag{3.2}$$

- We also use the following notation:

$$\begin{aligned}
&\mathcal{E}_h^I := \text{set of all interior edges/faces of } \mathcal{Q}_h,\\
&\mathcal{E}_h^R(\mathcal{E}_h^B) := \text{set of all boundary edges/faces of } \ \mathcal{Q}_h \text{ on } \Gamma_R(\Gamma_B),\\
&\mathcal{E}_h^{IB} := \mathcal{E}_h^I\cup\mathcal{E}_h^B \text{set of all edges/faces of } \ \mathcal{Q}_h \text{ except those on } \Gamma_R.
\end{aligned}$$

- Define the jump $[v]$ and average $\{v\}$ of v on an interior edges/face $e=\partial K_i\cap\partial K_j$ as

$$[v]|_e=\begin{cases} v|_{K_i}-v|_{K_j}, \text{ if the global label } i>j,\\[2mm] v|_{K_j}-v|_{K_i}, \text{ otherwise.}\end{cases} \tag{3.3}$$

  If $e\in\mathcal{E}_h^B$, we set $[v]|_e=v|_e$. The average is defined as follows

$$\{v\}|_e=\frac{1}{2}\big(v|_{K_i}+v|_{K_j}\big), \quad \text{if } e=\partial K_i\cap\partial K_j. \tag{3.4}$$

  If $e\in\mathcal{E}_h^B$ or $e\in\mathcal{E}_h^R$, set $\{v\}|_e=v|_e$. For every $e=\partial K_i\cap\partial K_j\in\mathcal{E}_h^I$, let $\boldsymbol{n}_e$ be the unit normal on edge/face e pointing from K_i to K_j if $i>j$ and from K_j to K_i otherwise. For every $e\in\mathcal{E}_h^R\cup\mathcal{E}_h^B$, let $\boldsymbol{n}_e=\boldsymbol{n}_\Omega$ be the unit outer normal of $\partial\Omega$.

- Define the sesquilinear form

$$a(w,v)=b(w,v)-\mathrm{i}\Big(J_0(w,v)+\sum_{j=1}^{q}J_j(w,v)\Big), \quad \forall\, w,v\in\mathcal{S}^q, \tag{3.5}$$

where

$$b(w,v)=\sum_{K\in\mathcal{Q}_h}(\nabla w,\nabla v)_K-\sum_{e\in\mathcal{E}_h^{IB}}\Big(\Big\langle\Big\{\frac{\partial w}{\partial \boldsymbol{n}_e}\Big\},[v]\Big\rangle_e+\sigma\Big\langle\Big\{\frac{\partial v}{\partial \boldsymbol{n}_e}\Big\},[w]\Big\rangle_e\Big),$$

$$J_0(w,v)=\sum_{e\in\mathcal{E}_h^{IB}}\frac{\gamma_{0,e}N_e}{|e|}\langle[w],[v]\rangle_e,$$

$$J_j(w,v)=\sum_{e\in\mathcal{E}_h^{I}}\gamma_{j,e}\Big(\frac{|e|}{N_e}\Big)^{2j-1}\Big\langle\Big[\frac{\partial^j w}{\partial \boldsymbol{n}_e^j}\Big],\Big[\frac{\partial^j v}{\partial \boldsymbol{n}_e^j}\Big]\Big\rangle_e,$$

where σ is a real number; $\gamma_{0,e}$, $\gamma_{1,e}$, $\cdots$, $\gamma_{q,e}$ are numbers to be defined later, $\frac{\partial^j w}{\partial \boldsymbol{n}_e^j}$ denotes the jth order normal derivative of w on e, and N_e is the largest degree of polynomial on the elements associated with e.

- Introduce the semi-norms on the space $\mathcal{S}^q$:

$$|v|_{1,\mathcal{Q}_h}:=\Big(\sum_{K\in\mathcal{Q}_h}\|\nabla v\|^2_{L^2(K)}\Big)^{\frac{1}{2}}, \tag{3.6}$$

$$\|v\|_{1,N,q}:=\Big(|v|^2_{1,\mathcal{Q}_h}+\sum_{e\in\mathcal{E}_h^{IB}}\frac{\gamma_{0,e}N_e}{|e|}\|[v]\|^2_{L^2(e)}+\sum_{j=1}^{q}\sum_{e\in\mathcal{E}_h^{I}}\gamma_{j,e}\Big(\frac{|e|}{N_e}\Big)^{2j-1}\Big\|\Big[\frac{\partial^j v}{\partial \boldsymbol{n}_e^j}\Big]\Big\|^2_{L^2(e)}\Big)^{\frac{1}{2}}, \tag{3.7}$$

$$|||v|||_{1,N,q}:=\Big(\|v\|^2_{1,N,q}+\sum_{e\in\mathcal{E}_h^{IB}}\frac{|e|}{\gamma_{0,e}N_e}\Big\|\Big\{\frac{\partial v}{\partial \boldsymbol{n}_e}\Big\}\Big\|^2_{L^2(e)}\Big)^{\frac{1}{2}}. \tag{3.8}$$

It is easy to check that for any $v\in\mathcal{S}^q$,

$$\mathrm{Re}\big(a(v,v)\big)=|v|^2_{1,\mathcal{Q}_h}-2\mathrm{Re}\sum_{e\in\mathcal{E}_h^{IB}}\Big\langle\Big\{\frac{\partial v}{\partial \boldsymbol{n}_e}\Big\},[v]\Big\rangle, \tag{3.9}$$

$$\mathrm{Im}\big(a(v,v)\big)=-(J_0(v,v)+J_1(v,v)+\cdots+J_q(v,v)). \tag{3.10}$$

The IPDG weak formulation for (2.9) is to find $u^{n+1}\in\mathcal{S}^q$ such that

$$a(u^{n+1},v)-k^2(u^{n+1},v)+kD_k\langle u^{n+1},v\rangle_{\Gamma_R}=(f,v)+\langle\delta_k u^n,v\rangle_{\Gamma_R},\quad \forall\, v\in\mathcal{S}^q, \tag{3.11}$$

where $\delta_k = kD_k - T$ as before. The parameter σ in $a(\cdot,\cdot)$ may take the value -1, 0 or 1. Correspondingly, the formulation (3.11) is referred to as the symmetric interior penalty Galerkin (SIPG) scheme if $\sigma=1$; the nonsymmetric interior penalty Galerkin scheme (NIPG) if $\sigma=-1$; or the incomplete interior penalty Galerkin scheme (IIPG) if $\sigma=0$, see [31]. Here, we restrict our attention to the SIPG case, i.e., $\sigma=1$.

For any $K\in\mathcal{Q}_h$, let $\mathbb{P}_p(K)$ be the set of all polynomials of degree at most p on K. We introduce the (IPDG) approximation space V_N as

$$V_N:=\big\{v\in L^2(\Omega): v|_{K_i}\in\mathbb{P}_{p_i}(K_i)\big\}, \tag{3.12}$$

where $N=\max\{p_i\geq 1: 1\leq i\leq N_h\}$ and N_h is the element number of the partition $\mathcal{Q}_h$. Suppose that the p-quasi-uniformity assumption holds, that is, the degree p_i on any element K_i satisfies

$$\frac{\max p_i}{\min p_i}\leq C_Q,\quad 1\leq i\leq N_h,$$

where the positive constant C_Q is independent of $|e|$ and N.

The multi-domain spectral IPDG method is to find $u_N^{n+1} \in V_N$ such that

$$a_N(u_N^{n+1}, v_N) - k^2(u_N^{n+1}, v_N) + kD_k\langle u_N^{n+1}, v_N\rangle_{\Gamma_R} = \langle f, v_N\rangle + \langle \delta_k u_N^n, v_N\rangle_{\Gamma_R}, \quad \forall\, v_N \in V_N, \tag{3.13}$$

where $a_N(u_N^{n+1}, v_N) = a(u_N^{n+1}, v_N)$ and the choice of D_k and R is strictly satisfying the convergence of the iterative scheme (2.9).

We state the following continuity and coercivity properties for the sesquilinear form $a(\cdot,\cdot)$, which follows from (3.5)-(3.10). For any $w,\, v \in \mathcal{S}^q$, the sesquilinear form $a(\cdot,\cdot)$ satisfies

$$|a(v,w)|,\ |a(w,v)| \lesssim \|v\|_{1,N,q}|||w|||_{1,N,q}. \tag{3.14}$$

Here and in the remainder of this work $A \lesssim B$ and $A \gtrsim B$ is used instead of $A \le CB$ and $A \ge CB$, respectively, for some positive generic constant C independent of N and q. And $A \simeq B$ is a shorthand notation for the statement $A \lesssim B$ and $B \lesssim A$.

For any $0 < \epsilon < 1$, there exists a positive constant C_ϵ depending on ϵ and independent of k, N and the penalty parameters such that $\forall\, v_N \in V_N$,

$$\mathrm{Re}\big(a_N(v_N, v_N)\big) - \Big(1 - \epsilon + \frac{C_\epsilon N}{\gamma_0}\Big)\mathrm{Im}\big(a_N(v_N, v_N)\big) \gtrsim (1-\epsilon)\|v_N\|_{1,N,q}^2, \tag{3.15}$$

where $\gamma_0 = \min\limits_{e\in\mathcal{E}_h^{IB}}\{\gamma_{0,e}\}$. Indeed, one just needs to prove

$$\epsilon|v_N|_{1,\mathcal{Q}_h}^2 - 2\mathrm{Re}\Big(\sum_{e\in\mathcal{E}_h^{IB}} \Big\langle\Big\{\frac{\partial v_N}{\partial \boldsymbol{n}_e}\Big\}, [v_N]\Big\rangle_e\Big) + \frac{C_\epsilon N}{\gamma_0}\sum_{j=0}^{q} J_j(v_N, v_N) \ge 0,$$

which follows from the Cauchy-Schwarz inequality applied to the second term of the above inequality.

Taking $v_n = u_N^{n+1}$ in (3.13), and taking real part and imaginary part of the resulted equation, we obtain the following lemma.

Lemma 3.1. *Let $u_N^{n+1} \in V_N$ be a solution to* (3.13)*. Then we have*

$$\begin{aligned} &\big|u_N^{n+1}\big|_{1,\mathcal{Q}_h}^2 - 2\mathrm{Re}\Big(\sum_{e\in\mathcal{E}_h^{IB}}\Big\langle\Big\{\frac{\partial u_N^{n+1}}{\partial \boldsymbol{n}_e}\Big\}, [u_N^{n+1}]\Big\rangle_e\Big) - k^2\big\|u_N^{n+1}\big\|_{L^2(\Omega)}^2 \\ &\quad + k\mathrm{Re}(D_k)\big\|u_N^{n+1}\big\|_{L^2(\Gamma_R)}^2 \le \Big|\mathrm{Re}\Big((f, u_N^{n+1}) + \langle\delta_k u_N^n, u_N^{n+1}\rangle_{\Gamma_R}\Big)\Big|, \end{aligned} \tag{3.16}$$

and

$$\begin{aligned} &\sum_{e\in\mathcal{E}_h^{IB}}\frac{\gamma_{0,e}N}{|e|}\big\|[u_N^{n+1}]\big\|_{L^2(e)}^2 + k|\mathrm{Im}(D_k)|\big\|u_N^{n+1}\big\|_{L^2(\Gamma_R)}^2 \\ &\quad + \sum_{j=1}^{q}\sum_{e\in\mathcal{E}_h^{I}}\gamma_{j,e}\Big(\frac{|e|}{N}\Big)^{2j-1}\Big\|\Big[\frac{\partial^j u_N^{n+1}}{\partial \boldsymbol{n}_e^j}\Big]\Big\|_{L^2(e)}^2 \le \Big|\mathrm{Im}\Big((f, u_N^{n+1}) + \langle\delta_k u_N^n, u_N^{n+1}\rangle_{\Gamma_R}\Big)\Big|. \end{aligned} \tag{3.17}$$

The following local Rellich lemma in [15] will be used in our analysis.

Lemma 3.2. *Let* $\alpha(x) := x - x_B, v \in \mathcal{S}^1, K, K' \in \mathcal{Q}_h$ *and* $e \in \mathcal{E}_h^{IB}$. *Then there hold*

$$d\|v\|^2_{L^2(K)} + 2\mathrm{Re}(v, \alpha\cdot\nabla v)_K = \int_{\partial K} \alpha\cdot\boldsymbol{n}_{\partial K}|v|^2 ds, \tag{3.18}$$

$$(d-2)\|\nabla v\|^2_{L^2(K)} + 2\mathrm{Re}(\nabla v, \nabla(\alpha\cdot\nabla v))_K = \int_{\partial K} \alpha\cdot\boldsymbol{n}_{\partial K}|\nabla v|^2 ds, \tag{3.19}$$

$$\begin{aligned}&\Big\langle\Big\{\frac{\partial v}{\partial \boldsymbol{n}_e}\Big\}, [\alpha\cdot\nabla v]\Big\rangle_e - \Big\langle \alpha\cdot\boldsymbol{n}_e\{\nabla v\}, [\nabla v]\Big\rangle_e\\ &\qquad = \sum_{l=1}^{d-1}\int_e \Big(\alpha\cdot\tau_e^l\Big\{\frac{\partial v}{\partial \boldsymbol{n}_e}\Big\} - \alpha\cdot\boldsymbol{n}_e\Big\{\frac{\partial v}{\partial \tau_e^l}\Big\}\Big)\Big[\frac{\partial \bar v}{\partial \tau_e^l}\Big] ds,\end{aligned} \tag{3.20}$$

where $d = 2, 3$, $\{\tau_e^l\}_{l=1}^{d-1}$ *is an orthogonal coordinate frame on the edge/face* $e \in \mathcal{E}_h$; *and* $\frac{\partial \bar v}{\partial \tau_e^l} := \nabla v\cdot\tau_e^l$ *is tangential derivative of* v *in the direction* τ_e^l.

We will also use the following discrete trace and inverse inequalities. In view of (3.2), for any $K \in \mathcal{Q}_h$ and $z \in \mathbb{P}_p(K)$, the following results hold:

$$\|z\|_{L^2(\partial K)} \lesssim p h_K^{-1/2}\|z\|_{L^2(K)} \lesssim p|e|^{-1/2}\|z\|_{L^2(K)}, \tag{3.21}$$

$$\|\nabla z\|_{L^2(K)} \lesssim p^2 h_K^{-1}\|z\|_{L^2(K)} \lesssim p^2|e|^{-1}\|z\|_{L^2(K)}. \tag{3.22}$$

4. Stability Analysis and Error Estimates

This section is devoted to the stability analysis of the IPDG scheme (3.13) at each iteration, and error estimates of the full scheme.

Theorem 4.1. *Let* $u_N^{n+1} \in V_N$ *solve* (3.13) *and suppose the penalty parameters* $\gamma_{i,e} > 0$, *for any* $0 \le i \le q$. *Then*

$$\begin{aligned}&\big\|u_N^{n+1}\big\|_{L^2(\Omega)} + \frac{1}{k}\big|u_N^{n+1}\big|_{1,\mathcal{Q}_h} + \frac{1}{k}\Big(C_{\Omega_R}\sum_{e\in\mathcal{E}_h^R}\big\|\nabla u_N^{n+1}\big\|^2_{L^2(e)}\Big)^{1/2}\\ &+\Big(\frac{\mathrm{Re}(D_k)}{k}\sum_{e\in\mathcal{E}_h^R}\big\|u_N^{n+1}\big\|^2_{L^2(e)}\Big)^{1/2} + \frac{1}{k}\Big(C_B\sum_{e\in\mathcal{E}_h^B}\Big(k^2\big\|u_N^{n+1}\big\|^2_{L^2(e)} + \frac{1}{2}\big\|\nabla u_N^{n+1}\big\|^2_{L^2(e)}\Big)\Big)^{1/2}\\ &\lesssim C_{stab}M(f, \delta_k u_N^n),\end{aligned} \tag{4.1}$$

where $M(f, \delta_k u_N^n) := \|f\|_{L^2(\Omega)} + \|\delta_k u_N^n\|_{L^2(\Gamma_R)}$, *and*

$$\begin{aligned}C_{stab} :=&\frac{1}{k|\mathrm{Im}(D_k)|} + \frac{1}{k^2}\max_{1\le j\le q}\Big(1 + \frac{N}{\gamma_{0,e}} + \gamma_{0,e}N + \sqrt{\gamma_{0,e}}N + N^2 + \frac{N^5}{\gamma_{0,e}}\Big)\\ &+\begin{cases}\frac{1}{k^2}\max\limits_{1\le j\le q}\Big(\sqrt{\frac{\gamma_{j,e}}{\gamma_{j+1,e}}}N + N^2 + \gamma_{q,e}N^{2q+3}\Big), & \textit{if}\quad q < N,\\ \frac{N}{k^2}\max\limits_{1\le j\le q}\Big(\sqrt{\frac{\gamma_{j,e}}{\gamma_{j+1,e}}} + N\Big), & \textit{if}\quad q \ge N.\end{cases}\end{aligned}$$

Proof. Following the argument used in Theorem 3.1 in [16] and Lemma 3.1 in [35], we sketch the derivation of this estimate in Appendix A. □

Remark 4.1. Under the assumption of quasi-uniformity of the mesh, we can write $\gamma_{j,e} \backsimeq \gamma_j$, $0 \le j \le q$ on all edges. Based on the estimates, we may analyze the choice of penalty parameters. To minimize the stability constant C_{stab}, we may choose $\gamma_0 \backsimeq N^2$, $\gamma_j \backsimeq N^{-1-2j}$, for $1 \le j \le q$, so that

$$C_{stab} \sim \frac{1}{k|\mathrm{Im}(D_k)|} + \frac{N^3}{k^2} + \frac{N^2}{k^2}. \tag{4.2}$$

With the aid of *a priori* error estimates, we analyze the convergence of the full scheme. Define the error function $e_N^{n+1} := u^{n+1} - u_N^{n+1}$, where u^{n+1} and u_N^{n+1} are the solutions of (2.9) and (3.13), respectively. Assuming that $u^{n+1} \in H^s(\Omega)$ with $s \ge q+1$, the variational formula (3.11) holds for $v_N \in V_N$. Subtracting (3.13) from (3.11) yields the error equation:

$$a_N(e_N^{n+1}, v_N) - k^2(e_N^{n+1}, v_N) + kD_k\langle e_N^{n+1}, v_N\rangle_{\Gamma_R} = \langle \delta_k e_N^n, v_N\rangle_{\Gamma_R}, \quad \forall v_N \in V_N. \tag{4.3}$$

We also suppose that the following Poisson problem is H^2-regular in the sense that for any $\psi \in L^2(\Omega)$ there is a unique $\phi \in H^2(\Omega)$ such that

$$\begin{cases} -\Delta\phi = \psi, & \text{in} \quad \Omega, \\ \phi = 0, & \text{on} \quad \Gamma_B, \\ \phi_r + kD_k\phi = 0, & \text{on} \quad \Gamma_R \end{cases} \tag{4.4}$$

and

$$|\phi|_{H^2(\Omega)} \lesssim k\|\psi\|_{L^2(\Omega)}. \tag{4.5}$$

Theorem 4.2. *Suppose that* $\gamma_0 \backsimeq N^2$, $\gamma_j \backsimeq N^{-1-2j}$, *for* $1 \le j \le q < \mu := \min\{N+1, s\}$. *Assume that the problem* (2.9) *is* H^s*-regular and* $u^m \in H^s(\Omega)$ *for* $0 \le m \le n+1$. *Let* u^{n+1} *and* u_N^{n+1} *be the solutions of* (2.9) *and* (3.13), *respectively. Then the following error estimate holds*

$$\begin{aligned} &\left\|e_N^{n+1}\right\|_{L^2(\Omega)} + \frac{1}{k}\left|e_N^{n+1}\right|_{1,\mathcal{Q}_h} + \frac{C_{\Omega_R}^{\frac{1}{2}}}{k}\left\|\nabla e_N^{n+1}\right\|_{L^2(\Gamma_R)} + \Big(\frac{\mathrm{Re}(D_K)}{k}\Big)^{\frac{1}{2}}\left\|e_N^{n+1}\right\|_{L^2(\Gamma_R)} \\ &\lesssim B_{k,N} N^{\frac{1}{2}-s}, \end{aligned} \tag{4.6}$$

where

$$B_{k,N} := \Big(k^{\frac{5}{2}} + k^{\frac{3}{2}}N^3 + k^{\frac{3}{2}}N^2 + 1 + k^{\frac{3}{2}} + C_{\Omega_R}^{\frac{1}{2}} k^{-\frac{1}{2}} N\Big) \sum_{m=0}^{n+1} \|u^m\|_{H^s(\Omega)}.$$

Proof. Let $\tilde{u}_N^{n+1}$ be the elliptic projection of u^{n+1} such that

$$a_N(u^{n+1}, v_N) + kD_k\langle u^{n+1}, v_N\rangle_{\Gamma_R} = a_N(\tilde{u}_N^{n+1}, v_N) + kD_k\langle \tilde{u}_N^{n+1}, v_N\rangle_{\Gamma_R}, \quad \forall\, v_N \in V_N. \tag{4.7}$$

We write $e_N^{n+1} = \chi^{n+1} - \xi^{n+1}$ with

$$\chi^{n+1} := u^{n+1} - \tilde{u}_N^{n+1}, \qquad \xi^{n+1} := u_N^{n+1} - \tilde{u}_N^{n+1}.$$

Without loss of generality, we assume that $\xi^0 = 0$ and $\nabla\xi^0 = 0$ on Γ_R. It follows from (4.3) and (4.7) that

$$a_N(\xi^{n+1}, v_N) - k^2(\xi^{n+1}, v_N) + kD_k\langle \xi^{n+1}, v_N\rangle_{\Gamma_R} = -k^2(\chi^{n+1}, v_N) - \langle \delta_k e_N^n, v_N\rangle_{\Gamma_R}, \tag{4.8}$$

which implies that $\xi^{n+1} \in V_N$ is the solution of the IPDG scheme (3.13) with $f = -k^2\chi^{n+1}$ and $\delta_k u_N^n$ replaced by $-\delta_k e_N^n$. Under the assumptions (4.4)-(4.5), analogously to Lemma 4.4 in [16], we have

$$\left\|\chi^{n+1}\right\|_{1,N,q} + \sqrt{k|D_k|}\left\|\chi^{n+1}\right\|_{L^2(\Gamma_R)} \lesssim C_{1,q}\Big(\frac{1}{N}\Big)^{s-1}\left\|u^{n+1}\right\|_{H^s(\Omega)}, \tag{4.9}$$

$$\left\|\nabla\chi^{n+1}\right\|_{1,N,q} + \sqrt{k|D_k|}\left\|\nabla\chi^{n+1}\right\|_{L^2(\Gamma_R)} \lesssim C_{1,q}\Big(\frac{1}{N}\Big)^{s-2}\left\|u^{n+1}\right\|_{H^s(\Omega)}, \tag{4.10}$$

$$\|\chi^{n+1}\|_{L^2(\Omega)} \lesssim C_{2,q}\Big(\frac{1}{N}\Big)^{s-1}\|u^{n+1}\|_{H^s(\Omega)}, \tag{4.11}$$

where

$$C_{1,q} = k^{1/2}\Big(\Big(1+\frac{N}{\gamma_0}\Big)^2\Big(1+\frac{N}{\gamma_0}+\sum_{j=1}^{q}N^{2j-1}\gamma_j\Big) + \Big(1+\frac{N}{\gamma_0}\Big)\frac{k|D_k|}{N}\Big)^{1/2},$$

$$C_{2,q} = k^{1/2}\Big(1+\frac{1}{\gamma_0 N}+\frac{\gamma_1}{N}+k|D_k|\Big)^{1/2}C_{1,q}.$$

Then applying Theorem 4.1 and (4.11) to (4.8) yields

$$\begin{aligned}&\left\|\xi^{n+1}\right\|_{L^2(\Omega)} + \frac{1}{k}\left|\xi^{n+1}\right|_{1,\mathcal{Q}_h} + \frac{C_{\Omega_R}^{\frac{1}{2}}}{k}\left\|\nabla\xi^{n+1}\right\|_{L^2(\Gamma_R)} + \Big(\frac{\mathrm{Re}(D_K)}{k}\Big)^{\frac{1}{2}}\left\|\xi^{n+1}\right\|_{L^2(\Gamma_R)}\\ \lesssim &C_{stab}\Big(C_{2,q}k^2\Big(\frac{1}{N}\Big)^{s-1}\left\|u^{n+1}\right\|_{H^s(\Omega)} + \|\delta_k e_N^n\|_{L^2(\Gamma_R)}\Big).\end{aligned} \tag{4.12}$$

We now estimate $\|\delta_k e_N^n\|_{L^2(\Gamma_R)}$. Similar to the estimate (2.34), $\|\delta_k e_N^n\|_{L^2(\Gamma_R)}$ can be bounded by

$$\begin{aligned}\|\delta_k e_N^n\|_{L^2(\Gamma_R)} &\le k|\delta_{0,kR}|\,\|e_N^n\|_{L^2(\Gamma_R)} + k\max_{|m|\neq 0}\big\{|m|^{-1}\delta_{m,kR}\big\}\,\|\nabla_T e_N^n\|_{L^2(\Gamma_R)}\\ &\le k|\delta_{0,kR}|\big(\|\xi^n\|_{L^2(\Gamma_R)} + \|\chi^n\|_{L^2(\Gamma_R)}\big)\\ &\quad + k\max_{|m|\neq 0}\big\{|m|^{-1}\delta_{m,kR}\big\}\big(\|\nabla\xi^n\|_{L^2(\Gamma_R)} + \|\nabla\chi^n\|_{L^2(\Gamma_R)}\big)\\ &\lesssim k|\delta_{0,kR}|\,\|\xi^n\|_{L^2(\Gamma_R)} + k\max_{|m|\neq 0}\big\{|m|^{-1}\delta_{m,kR}\big\}\,\|\nabla\xi^n\|_{L^2(\Gamma_R)}\\ &\quad + |\delta_{0,kR}|k^{\frac{1}{2}}|D_k|^{-\frac{1}{2}}C_{1,q}N^{1-s}\,\|u^n\|_{H^s(\Omega)}\\ &\quad + k^{\frac{1}{2}}|D_k|^{-\frac{1}{2}}\max_{|m|\neq 0}\big\{|m|^{-1}\delta_{m,kR}\big\}C_{1,q}N^{2-s}\,\|u^n\|_{H^s(\Omega)},\end{aligned} \tag{4.13}$$

where in the last step, we used the estimates (4.9)-(4.10).

On the one hand, by (4.12) and (4.13), it holds that

$$\begin{aligned}&\left\|\xi^{n+1}\right\|_{L^2(\Omega)} + \frac{1}{k}\left|\xi^{n+1}\right|_{1,\mathcal{Q}_h} + \frac{C_{\Omega_R}^{\frac{1}{2}}}{k}\left\|\nabla\xi^{n+1}\right\|_{L^2(\Gamma_R)} + \Big(\frac{\mathrm{Re}(D_K)}{k}\Big)^{\frac{1}{2}}\left\|\xi^{n+1}\right\|_{L^2(\Gamma_R)}\\ \lesssim\ &C_{stab}k|\delta_{0,kR}|\,\|\xi^n\|_{L^2(\Gamma_R)} + C_{stab}k\max_{|m|\neq 0}\big\{|m|^{-1}\delta_{m,kR}\big\}\,\|\nabla\xi^n\|_{L^2(\Gamma_R)}\\ &+ C_{stab}C_{2,q}k^2N^{1-s}\left\|u^{n+1}\right\|_{H^s(\Omega)} + C_{stab}|\delta_{0,kR}|k^{\frac{1}{2}}|D_k|^{-\frac{1}{2}}C_{1,q}N^{1-s}\,\|u^n\|_{H^s(\Omega)}\\ &+ C_{stab}k^{\frac{1}{2}}|D_k|^{-\frac{1}{2}}\max_{|m|\neq 0}\big\{|m|^{-1}\delta_{m,kR}\big\}C_{1,q}N^{2-s}\,\|u^n\|_{H^s(\Omega)}.\end{aligned} \tag{4.14}$$

Note that

$$C_{1,q} \lesssim kN^{-\frac{1}{2}}, \quad C_{2,q} \lesssim k^{\frac{3}{2}}N^{-\frac{1}{2}}, \quad C_{stab} \lesssim k^{-1} + N^3k^{-2} + N^2k^{-2}.$$

It follows from the previous three cases of D_k that

$$|\delta_{0,kR}| \lesssim \frac{1}{kR}, \quad \max_{|m|\neq 0}\left\{|m|^{-1}\delta_{m,kR}\right\} \lesssim \frac{1}{kR}.$$

We give a preasymptotic error estimate for a fixed D_k with an appropriate choice of R

$$\begin{aligned}
&\left\|\xi^{n+1}\right\|_{L^2(\Omega)} + \frac{1}{k}\left|\xi^{n+1}\right|_{1,\mathcal{Q}_h} + \frac{C_{\Omega_R}^{\frac12}}{k}\left\|\nabla\xi^{n+1}\right\|_{L^2(\Gamma_R)} + \Big(\frac{\mathrm{Re}(D_K)}{k}\Big)^{\frac12}\left\|\xi^{n+1}\right\|_{L^2(\Gamma_R)}\\
\lesssim&\frac{C_{\Omega_R}^{\frac12}}{k}\left\|\nabla\xi^{n}\right\|_{L^2(\Gamma_R)} + \Big(\frac{\mathrm{Re}(D_K)}{k}\Big)^{\frac12}\left\|\xi^{n}\right\|_{L^2(\Gamma_R)} + C_{stab}k^{\frac72}N^{\frac12-s}\left\|u^{n+1}\right\|_{H^s(\Omega)}\\
&+N^{\frac12-s}\left\|u^{n}\right\|_{H^s(\Omega)} + C_{\Omega_R}^{\frac12}k^{-\frac12}N^{\frac32-s}\left\|u^{n}\right\|_{H^s(\Omega)}.
\end{aligned}\tag{4.15}$$

By deduction and the assumption of ξ^0 and $\nabla\xi^0$ on Γ_R, (4.15) becomes

$$\begin{aligned}
&\|\xi^{n+1}\|_{L^2(\Omega)} + \frac{1}{k}\left|\xi^{n+1}\right|_{1,\mathcal{Q}_h} + \frac{C_{\Omega_R}^{\frac12}}{k}\|\nabla\xi^{n+1}\|_{L^2(\Gamma_R)} + \Big(\frac{\mathrm{Re}(D_K)}{k}\Big)^{\frac12}\|\xi^{n+1}\|_{L^2(\Gamma_R)}\\
\lesssim&(k^{-1}+k^{-2}N^3+N^2k^{-2})k^{\frac72}N^{\frac12-s}\sum_{m=1}^{n+1}\|u^m\|_{H^s(\Omega)}\\
&+\Big(1+C_{\Omega_R}^{\frac12}k^{-\frac12}N\Big)N^{\frac12-s}\sum_{m=0}^{n}\|u^m\|_{H^s(\Omega)}.
\end{aligned}\tag{4.16}$$

On the other hand, combining (4.11) with (4.10) leads to

$$\begin{aligned}
&\left\|\chi^{n+1}\right\|_{L^2(\Omega)} + \frac{1}{k}\left\|\chi^{n+1}\right\|_{1,N,q} + \frac{C_{\Omega_R}^{\frac12}}{k}\left\|\nabla\chi^{n+1}\right\|_{L^2(\Gamma_R)} + \Big(\frac{\mathrm{Re}(D_K)}{k}\Big)^{\frac12}\left\|\chi^{n+1}\right\|_{L^2(\Gamma_R)}\\
\lesssim&\Big(k^{-1}C_{1,q}N^{1-s} + C_{2,q}N^{1-s} + C_{\Omega_R}^{\frac12}k^{-\frac32}C_{1,q}N^{2-s}\Big)\left\|u^{n+1}\right\|_{H^s(\Omega)}\\
\lesssim&\Big(1+k^{\frac32}+C_{\Omega_R}^{\frac12}k^{-\frac12}N\Big)N^{\frac12-s}\left\|u^{n+1}\right\|_{H^s(\Omega)}.
\end{aligned}\tag{4.17}$$

Notice that $\left|\chi^{n+1}\right|_{1,\mathcal{Q}_h} \leq \left\|\chi^{n+1}\right\|_{1,N,q}$. Adding (4.16)-(4.17) results in (4.6). □

Remark 4.2. Notice that the first three terms in $B_{k,N}$ indicate the "pollution errors" of the full DG iterative scheme.

Finally, by recalling Theorems 2.14 and 4.2, we have the DG approximation error bounds in the wave number dependent H^1-norm for the multi-domain spectral IPDG scheme (3.13) as a numerical approximation to the original problem (2.1).

Theorem 4.3. *Under the conditions of* Theorems 2.14 *and* 4.2*, we have the estimate*

$$\begin{aligned}
&|||u-u_N^n|||_{1,\Omega}^2 + k\mathrm{Re}(D_k)\|u-u_N^n\|_{L^2(\Gamma_R)}^2 + \min\{C_{\Omega_R},R\}\|\nabla_T(u-u_N^n)\|_{L^2(\Gamma_R)}^2\\
\lesssim&(S_1(k))^n\Big(Rk^2\mathrm{Im}(D_k)^2 + k\mathrm{Re}(D_k)\Big)\|e^0\|_{L^2(\Gamma_R)}^2\\
&+(S_2(k))^nR\|\nabla_Te^0\|_{L^2(\Gamma_R)}^2 + B_{k,N}^2k^2N^{1-2s},
\end{aligned}\tag{4.18}$$

where D_k is appropriately chosen such that $S_i(k) < 1$, $i = 1, 2$.

5. Numerical Results

We now present numerical results to demonstrate the convergence of the scheme (3.13). Let the scatterer B be an octagon with the length of each side being $2r\sin(\pi/8)$ (cf. Fig. 5.1 (b) for the definition of r). We plot in Fig. 5.1 (b) the partition of the computational domain Ω, and depict the grids on one element in Fig. 5.1(a).

$$\begin{cases} x = \dfrac{x_1}{4}(1-\xi)(1-\eta) + \dfrac{x_2}{4}(1+\xi)(1-\eta) \\ \qquad + \dfrac{Rc(\xi,x_3,x_4)}{2\sqrt{c^2(\xi,x_3,x_4)+d^2(\xi,x_3,x_4)}}(1+\eta), \\ y = \dfrac{y_1}{4}(1-\xi)(1-\eta) + \dfrac{y_2}{4}(1+\xi)(1-\eta) \\ \qquad + \dfrac{Rd(\xi,y_3,y_4)}{2\sqrt{c^2(\xi,y_3,y_4)+d^2(\xi,y_3,y_4)}}(1+\eta), \end{cases} \tag{5.1}$$

where

$$c(\xi,x_3,x_4) = \frac{x_3}{2}(1-\xi) + \frac{x_4}{2}(1+\xi), \quad d(\xi,y_3,y_4) = \frac{y_3}{2}(1-\xi) + \frac{y_4}{2}(1+\xi).$$

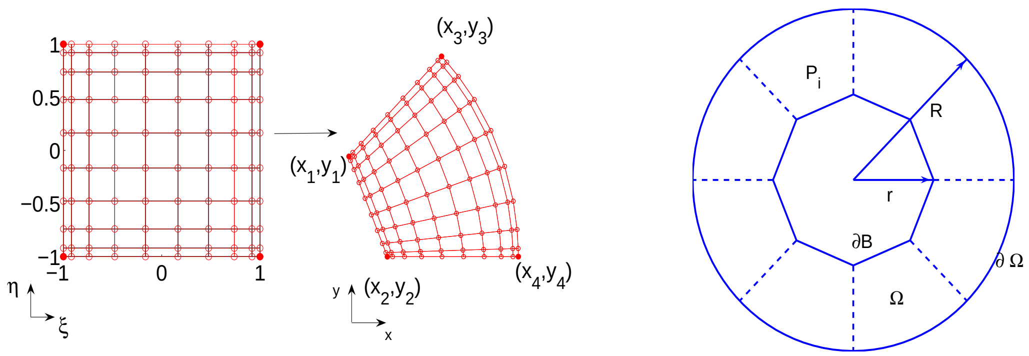

(a) (b)

Fig. 5.1. (a): grids on the reference square (left), and the curved element (right); (b): partition of the computational domain.

We first test the iterative p-IPDG solver (3.13) on a problem with exact solution. More precisely, we consider

$$\begin{cases} -\Delta u - k^2 u = f, & \text{in} \quad \Omega, \\ u = g, & \text{on} \quad \Gamma_B, \\ (\partial_r + kD_k)u = (kD_k - T)u + h, & \text{on} \quad \Gamma_R, \end{cases} \tag{5.2}$$

with the exact solution

$$u = \cos(\sqrt{x^2+y^2}) + \mathrm{i}\sin(\sqrt{x^2+y^2}),$$

where D_k and T are the same as before, and f, g and h are determined by exact solution.

In the computation, we evaluate the DtN operator T by a suitable truncation:

$$T_M u := -\sum_{l=-M}^{M} k \frac{\partial_z H_l^{(1)}(kR)}{H_l^{(1)}(kR)} \hat{u}_l(R) e^{\mathrm{i}l\theta}, \tag{5.3}$$

and adopt the stopping rule for the iteration: $\|u_N^{n+1} - u_N^n\|_\infty \le 10^{-10}$. We choose $M = 50, D_k = -T_{0,kR}$ and the penalization parameters are $\gamma_0 = N^2$ and $\gamma_1 = 1/N$.

In Table 5.1, we tabulate the number of iterations n, which is taken to meet the stopping rule, and the numerical errors: $E_{N,n} = \|u - u_N^n\|_\infty$ for various k and N, and two pairs of r and R. We see that as N increases, the errors decay very fast with a small amount of iterations.

Table 5.1: Convergence of the p-IPDG scheme.

$r = 0.3, R = 3$				$r = 0.2, R = 5$			
k	N	n	$E_{N,n}$	k	N	n	$E_{N,n}$
100	7	44	$2.82E-04$	70	7	18	$1.87E-02$
120	9	54	$1.25E-05$	100	9	21	$4.32E-04$
200	12	57	$8.08E-07$	120	12	34	$1.20E-06$
300	16	45	$8.48E-09$	200	16	33	$4.98E-09$

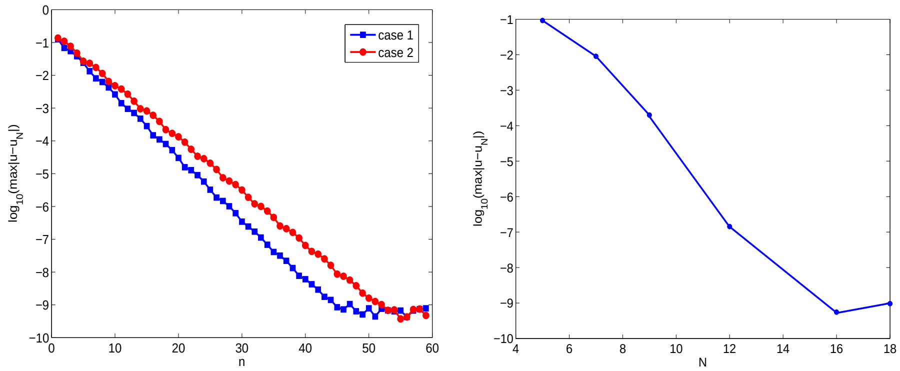

Fig. 5.2. Convergence of the p-IPDG scheme. Left: $\log_{10}(E_{N,n})$ against n for cases 1-2. Right: $\log_{10}(E_{N,n})$ against N, where $r = 0.2, R = 0.5, k = 200$.

To examine the history of convergence of the iterative scheme, we fix N and k, and record in Fig. 5.2 (left) $\log_{10}(E_{N,n})$ against n for the following two cases:

- *Case* 1. $r = 0.3, R = 3, k = 300, N = 16, \gamma_0 = N^2$ and $\gamma_1 = 1/N$.
- *Case* 2. $r = 0.2, R = 5, k = 200, N = 18, \gamma_0 = N^2$ and $\gamma_1 = 1/N$.

To check the convergence with respect to N, we plot in Fig. 5.2 (right) the error $\log_{10}(E_{N,n})$, at the iterative step n such that $\|u_N^{n+1} - u_N^n\|_\infty \le 10^{-10}$, against various N.

We observe from Fig. 5.2 that the iterative scheme converges fast in both n and N, and the scheme produces spectral accurate numerical results.

Finally, we consider the algorithm to solve the scattering problem (2.1) with the computational domain as in Fig. 5.1 (b), and with $g = 1/2$. Here, we choose the local operator $D_k = -T_{0,kR}$ and evaluate the DtN operator in the same way as before. In this case we don't have an exact solution.

In Fig. 5.3, we plot numerical solutions for the following setup:

- *Case* 3. $r = 0.3, R = 4, k = 240, N = 12, \gamma_0 = N^2$ and $\gamma_1 = 1/N$.

- *Case* 4. $r = 0.2, R = 5, k = 200, N = 16, \gamma_0 = N^2$ and $\gamma_1 = 1/N$.

We visualize from Fig. 5.3 that the waves (of ring-pattern in radial direction) propagate smoothly through the truncated boundary. We also compare the solution with the "reference solution" obtained by very fine mesh, and find that the accuracy is as expected.

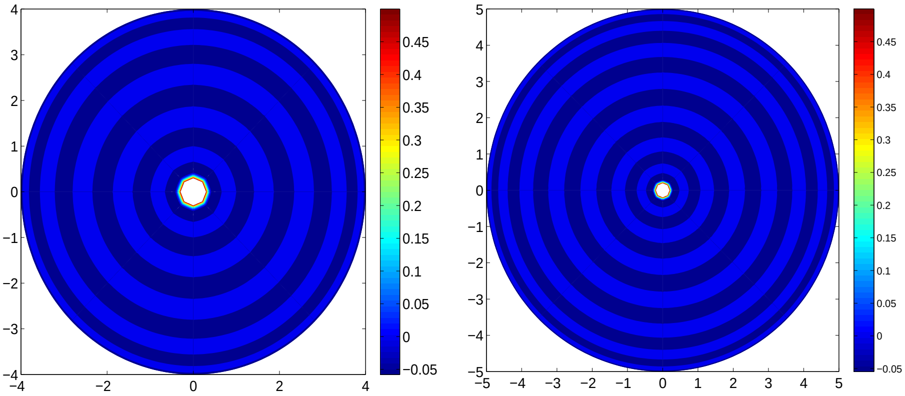

Fig. 5.3. Numerical solutions of the Helmholtz equation. Left: Case 3. Right: Case 4.

A. Proof of Theorem 4.1

Proof. For clarity, we separate the proof into several steps.

Step1: Derivation for $\|u_N^{n+1}\|_{L^2(\Omega)}$. On the one hand, taking $v_N = u_N^{n+1}$ in (3.13), we get the real part of the resulted equation as follows:

$$\begin{aligned} &-k^2 \|u_N^{n+1}\|^2_{L^2(\Omega)} \\ &= \mathrm{Re}\big((f, u_N^{n+1}) + \langle \delta_k u_N^n, u_N^n\rangle_{\Gamma_R} - a_N(u_N^{n+1}, u_N^{n+1}) - kD_k\langle u_N^{n+1}, u_N^{n+1}\rangle_{\Gamma_R}\big). \end{aligned} \tag{A.1}$$

On the other hand, we first define v_N by $v_N|_K = \alpha \cdot \nabla u_N^{n+1}|_K = (x - x_B)\cdot \nabla u_N^{n+1}|_K$ on every element $K \in \mathcal{Q}_h$, where $x_B \in B$. It is obvious that $v_N \in V_N$. Using v_N as a test function in (3.13) and taking the real part of the resulted equation, we get

$$\begin{aligned} &-2k^2 \mathrm{Re}(u_N^{n+1}, v_N) \\ &= 2\mathrm{Re}\big((f, v_N) + \langle \delta_k u_N^n, v_N\rangle_{\Gamma_R} - a_N(u_N^{n+1}, v_N) - kD_k\langle u_N^{n+1}, v_N\rangle_{\Gamma_R}\big). \end{aligned} \tag{A.2}$$

By adding k^2 times (3.18) with $v_N|_K = \alpha \cdot \nabla u_N^{n+1}|_K$ to (A.2) we have

$$\begin{aligned} 2k^2 \|u_N^{n+1}\|^2_{L^2(\Omega)} = & k^2 \sum_{K\in\mathcal{Q}_h} \int_{\partial K} \alpha \cdot \boldsymbol{n}_{\partial K} \left|u_N^{n+1}\right|^2 ds + 2\mathrm{Re}\big((f, v_N) \\ & + \langle \delta_k u_N^n, v_N\rangle_{\Gamma_R} - a_N(u_N^{n+1}, v_N) - kD_k\langle u_N^{n+1}, v_N\rangle_{\Gamma_R}\big). \end{aligned} \tag{A.3}$$

Therefore, adding $\frac{1}{8}$ times (A.1) to (A.3) gives

$$\begin{aligned} \frac{15}{8} k^2 \|u_N^{n+1}\|^2_{L^2(\Omega)} = & k^2 \sum_{K\in\mathcal{Q}_h} \int_{\partial K} \alpha \cdot \boldsymbol{n}_{\partial K} \left|u_N^{n+1}\right|^2 ds - \frac{1}{8} k\mathrm{Re}(D_k)\langle u_N^{n+1}, u_N^{n+1}\rangle_{\Gamma_R} \\ & + \frac{1}{8}\mathrm{Re}\big((f, u_N^{n+1}) + \langle \delta_k u_N^n, u_N^{n+1}\rangle_{\Gamma_R} - a_N(u_N^{n+1}, u_N^{n+1})\big) \\ & + 2\mathrm{Re}\big((f, v_N) + \langle \delta_k u_N^n, v_N\rangle_{\Gamma_R} - a_N(u_N^{n+1}, v_N) - kD_k\langle u_N^{n+1}, v_N\rangle_{\Gamma_R}\big). \end{aligned}$$

By (3.13), we get

$$
\begin{aligned}
&\frac{15}{8}k^2\left\|u_N^{n+1}\right\|_{L^2(\Omega)}^2\\
=&k^2\sum_{K\in\mathcal{Q}_h}\int_{\partial K}\alpha\cdot\boldsymbol{n}_{\partial K}|u_N^{n+1}|^2ds+\frac{1}{8}\mathrm{Re}\big((f,u_N^{n+1})+\langle\delta_k u_N^n,u_N^{n+1}\rangle_{\Gamma_R}\\
&-kD_k\langle u_N^{n+1},u_N^{n+1}\rangle_{\Gamma_R}\big)+2\mathrm{Re}\big((f,v_N)+\langle\delta_k u_N^n,v_N\rangle_{\Gamma_R}\big)-2k\mathrm{Re}\big(D_k\langle u_N^{n+1},v_N\rangle_{\Gamma_R}\big)\\
&-\sum_{K\in Q_h}\Big(\frac{1}{8}\left\|\nabla u_N^{n+1}\right\|_{L^2(K)}^2+2\mathrm{Re}(\nabla u_N^{n+1},\nabla v_N)\Big)\\
&+2\sum_{e\in\mathcal{E}_h^{IB}}\Big(\frac{1}{8}\mathrm{Re}\Big\langle\Big\{\frac{\partial u_N^{n+1}}{\partial\boldsymbol{n}_e}\Big\},[u_N^{n+1}]\Big\rangle_e+\mathrm{Re}\Big\langle\Big\{\frac{\partial u_N^{n+1}}{\partial\boldsymbol{n}_e}\Big\},[v_N]\Big\rangle_e\\
&+\mathrm{Re}\Big\langle\Big\{\frac{\partial v_N}{\partial\boldsymbol{n}_e}\Big\},[u_N^{n+1}]\Big\rangle_e\Big)-2\mathrm{Im}\big(J_0(u_N^{n+1},v_N)+\sum_{j=1}^{q}J_j(u_N^{n+1},v_N)\big).
\end{aligned}\tag{A.4}
$$

Using the identity $|a|^2-|b|^2=\mathrm{Re}(a+b)(\bar{a}-\bar{b})$, we have

$$
\sum_{K\in\mathcal{Q}_h}\int_{\partial K}\alpha\cdot\boldsymbol{n}_{\partial K}|u_N^{n+1}|^2ds=2\sum_{e\in\mathcal{E}_h^I}\mathrm{Re}\langle\alpha\cdot\boldsymbol{n}_e\{u_N^{n+1}\},[u_N^{n+1}]\rangle_e+\langle\alpha\cdot\boldsymbol{n}_e,|u_N^{n+1}|^2\rangle_{\partial\Omega}. \tag{A.5}
$$

Note that

$$
\boldsymbol{n}_{\partial K}=\begin{cases}\boldsymbol{n}_{\Gamma_B}, & \text{on}\quad\Gamma_B,\\ \boldsymbol{n}_{\Gamma_R}, & \text{on}\quad\Gamma_R,\end{cases}\qquad \begin{cases}\boldsymbol{n}_{\Gamma_B}=-\boldsymbol{n}_e, & \text{for any}\quad e\in\Gamma_B,\\ \boldsymbol{n}_{\Gamma_R}=\boldsymbol{n}_e, & \text{for any}\quad e\in\Gamma_R.\end{cases}
$$

From (3.19) and (A.5), we get

$$
\begin{aligned}
&\sum_{K\in\mathcal{Q}_h}2\mathrm{Re}(\nabla u_N^{n+1},\nabla v_N)_K=\sum_{K\in\mathcal{Q}_h}\int_{\partial K}\alpha\cdot\boldsymbol{n}_{\partial K}\left|\nabla u_N^{n+1}\right|^2ds\\
=&\ 2\sum_{e\in\mathcal{E}_h^{IB}}\mathrm{Re}\langle\alpha\cdot\boldsymbol{n}_e\{\nabla u_N^{n+1}\},[\nabla u_N^{n+1}]\rangle_e+\sum_{e\in\mathcal{E}_h^R}\langle\alpha\cdot\boldsymbol{n}_e,|\nabla u_N^{n+1}|^2\rangle_e\\
&-\sum_{e\in\mathcal{E}_h^B}\langle\alpha\cdot\boldsymbol{n}_e,|\nabla u_N^{n+1}|^2\rangle_e.
\end{aligned}\tag{A.6}
$$

Plugging (A.5) and (A.6) into (A.4) gives

$$
\begin{aligned}
\frac{15}{8}k^2\left\|u_N^{n+1}\right\|_{L^2(\Omega)}^2=&\frac{1}{8}\mathrm{Re}\big((f,v_N^{n+1})+\langle\delta_k u_N^n,u_N^{n+1}\rangle_{\Gamma_R}-k\mathrm{Re}(D_k)\langle u_N^{n+1},u_N^{n+1}\rangle_{\Gamma_R}\big)\\
&+2\mathrm{Re}\big((f,v_N)+\langle\delta_k u_N^n,v_N\rangle_{\Gamma_R}\big)\\
&+2k^2\sum_{e\in\mathcal{E}_h^I}\mathrm{Re}\langle\alpha\cdot\boldsymbol{n}_e\left\{u_N^{n+1}\right\},[u_N^{n+1}]\}\rangle_e+k^2\langle\alpha\cdot\boldsymbol{n}_e,\left|u_N^{n+1}\right|^2\rangle_{\partial\Omega}\\
&-\frac{1}{8}\sum_{K\in\mathcal{Q}_h}\left\|\nabla u_N^{n+1}\right\|_{L^2(k)}^2+\sum_{e\in\mathcal{E}_h^B}\langle\alpha\cdot\boldsymbol{n}_e,\left|\nabla u_N^{n+1}\right|^2\rangle_e+A_1+A_2\\
&-2\sum_{e\in\mathcal{E}_h^{IB}}\mathrm{Re}\Big\langle\Big\{\frac{\partial u_N^{n+1}}{\partial\boldsymbol{n}_e}\Big\},[u_N^{n+1}]\Big\rangle_e+\frac{9}{4}\sum_{e\in\mathcal{E}_h^{IB}}\Big\langle\Big\{\frac{\partial u_N^{n+1}}{\partial\boldsymbol{n}_e}\Big\},[u_N^{n+1}]\Big\rangle_e\\
&+2\sum_{e\in\mathcal{E}_h^{IB}}\mathrm{Re}\Big\langle\Big\{\frac{\partial v_N}{\partial\boldsymbol{n}_e}\Big\},[u_N^{n+1}]\Big\rangle_e-2\mathrm{Im}\Big(J_0(u_N^{n+1},v_N)+\sum_{j=1}^{q}J_j(u_N^{n+1},v_N)\Big),
\end{aligned}\tag{A.7}
$$

where

$$A1 = -2k\mathrm{Re}(D_k\langle u_N^{n+1}, v_N\rangle_{\Gamma_R}) - \sum_{e\in\mathcal{E}_h^R}\langle \alpha\cdot\boldsymbol{n}_e, |\nabla u_N^{n+1}|^2\rangle_e,$$

$$A2 = 2\sum_{e\in\mathcal{E}_h^{IB}}\mathrm{Re}\Big(-\Big\langle \alpha\cdot\boldsymbol{n}_e\{\nabla u_N^{n+1}\}, [\nabla u_N^{n+1}]\Big\rangle_e + \Big\langle\Big\{\frac{\partial u_N^{n+1}}{\partial\boldsymbol{n}_e}\Big\}, [v_N]\Big\rangle_e\Big).$$

Step 2: Let us estimate each term on the right-hand side of (A.7). Setting $M(f,\delta_k u_N^n) = \|f\|_{L^2(\Omega)} + \|\delta_k u_N^n\|_{L^2(\Gamma_R)}$, we derive the following estimates:

$$A_1 \le Ck^2\|u_N^{n+1}\|^2_{L^2(\Gamma_R)} - \frac{C_{\Omega_R}}{2}\sum_{e\in\mathcal{E}_h^R}\|\nabla u_N^{n+1}\|^2_{L^2(e)},$$

$$2\mathrm{Re}\big((f,v_N) + \langle\delta_k u_N^n, v_N\rangle_{\Gamma_R}\big) \le CM(f,\delta_k u_N^n)^2 + \frac{1}{8}\left|u_N^{n+1}\right|^2_{1,\mathcal{Q}_h} + \frac{C_{\Omega_R}}{4}\sum_{e\in\mathcal{E}_h^R}\left\|\nabla u_N^{n+1}\right\|^2_{L^2(e)},$$

$$2k^2\sum_{e\in\mathcal{E}_h^I}\mathrm{Re}\langle\alpha\cdot\boldsymbol{n}_e\{u_N^{n+1}\}, [u_N^{n+1}]\rangle_e \le Ck^2\sum_{e\in\mathcal{E}_h^I}N\left\|u_N^{n+1}\right\|_{L^2(K_e\cup K_{e'})}\left\|[u_N^{n+1}]\right\|_{L^2(e)} \tag{A.8}$$

$$\le \frac{k^2}{8}\left\|u_N^{n+1}\right\|^2_{L^2(\Omega)} + C\sum_{e\in\mathcal{E}_h^I}\frac{Nk^2|e|}{\gamma_{0,e}}\frac{\gamma_{0,e}N}{|e|}\left\|[u_N^{n+1}]\right\|^2_{L^2(e)}, \tag{A.9}$$

$$k^2\langle\alpha\cdot\boldsymbol{n}_e, \left|u_N^{n+1}\right|^2\rangle_{\partial\Omega} \le Ck^2\left\|u_N^{n+1}\right\|^2_{L^2(\Gamma_R)} + \sum_{e\in\mathcal{E}_h^B}k^2\langle\alpha\cdot\boldsymbol{n}_e, \left|u_N^{n+1}\right|^2\rangle_e.$$

For any $e\in\mathcal{E}_h^{IB}$, let Ω_e be the set of elements in Γ_h containing e. Then by (3.20),

$$\begin{aligned}
A_2 &= 2\sum_{e\in\mathcal{E}_h^{IB}}\sum_{l=1}^{d-1}\mathrm{Re}\int_e\Big(\alpha\cdot\tau_e^l\Big\{\frac{\partial u_N^{n+1}}{\partial\boldsymbol{n}_e}\Big\} - \alpha\cdot\boldsymbol{n}_e\Big\{\frac{\partial u_N^{n+1}}{\partial\tau_e^l}\Big\}\Big)\Big[\frac{\partial\bar{u}_N^{n+1}}{\partial\tau_e^l}\Big]ds\\
&\lesssim \sum_{e\in\mathcal{E}_h^{IB}}\sum_{l=1}^{d-1}N|e|^{-1/2}\sum_{K\in\Omega_e}\left\|\nabla u_N^{n+1}\right\|_{L^2(K)}\left\|\Big[\frac{\partial\bar{u}_N^{n+1}}{\partial\tau_e^l}\Big]\right\|_{L^2(e)}\\
&\lesssim \sum_{e\in\mathcal{E}_h^{IB}}N^3|e|^{-3/2}\sum_{K\in\Omega_e}\left\|\nabla u_N^{n+1}\right\|_{L^2(K)}\left\|[u_N^{n+1}]\right\|_{L^2(e)}\\
&\le \frac{1}{8}\left|u_N^{n+1}\right|^2_{1,\Omega} + C\sum_{e\in\mathcal{E}_h^{IB}}\frac{N^5}{\gamma_{0,e}|e|^2}\frac{\gamma_{0,e}N}{|e|}\left\|[u_N^{n+1}]\right\|^2_{L^2(e)}.
\end{aligned}$$

Thanks to the trace and inverse inequalities (3.21)-(3.22), we have

$$\begin{aligned}
2\sum_{e\in\mathcal{E}_h^{IB}}\mathrm{Re}\Big(\Big\langle\Big\{\frac{\partial v_N}{\partial\boldsymbol{n}_e}\Big\}, [u_N^{n+1}]\Big\rangle_e\Big) &\lesssim \sum_{e\in\mathcal{E}_h^{IB}}N|e|^{-1/2}\left\|[u_N^{n+1}]\right\|_{L^2(e)}\sum_{K\in\mathcal{Q}_h}\|\nabla v_N\|_{L^2(K)}\\
&\lesssim \sum_{e\in\mathcal{E}_h^{IB}}N^3|e|^{-3/2}\left\|[u_N^{n+1}]\right\|_{L^2(e)}\sum_{K\in\mathcal{Q}_h}\left\|\nabla u_N^{n+1}\right\|_{L^2(K)}\\
&\le \frac{1}{8}\left|u_N^{n+1}\right|^2_{1,\Omega} + C\sum_{e\in\mathcal{E}_h^{IB}}\frac{N^5}{\gamma_{0,e}|e|^2}\frac{\gamma_{0,e}N}{|e|}\left\|[u_N^{n+1}]\right\|^2_{L^2(e)},
\end{aligned}$$

$$\frac{9}{4}\sum_{e\in\mathcal{E}_h^{IB}}\mathrm{Re}\Big(\Big\langle\Big\{\frac{\partial u_N^{n+1}}{\partial\boldsymbol{n}_e}\Big\}, [u_N^{n+1}]\Big\rangle_e\Big) \le \frac{1}{8}\left|u_N^{n+1}\right|^2_{1,\Omega} + C\sum_{e\in\mathcal{E}_h^{IB}}\frac{N}{\gamma_{0,e}}\frac{\gamma_{0,e}N}{|e|}\left\|[u_N^{n+1}]\right\|^2_{L^2(e)}.$$

Recall that $v_N|_K = \alpha\cdot\nabla u_N^{n+1}|_K$ with $\alpha = x - x_B$ for each $K\in\mathcal{Q}_h$. Noting that

$$\begin{aligned}\frac{\partial v_N}{\partial \tau_e^l} =&\frac{\partial u_N^{n+1}}{\partial \tau_e^l} + \alpha\cdot\nabla\frac{\partial u_N^{n+1}}{\partial \tau_e^l}\\ =&\frac{\partial u_N^{n+1}}{\partial \tau_e^l} + \alpha\cdot\boldsymbol{n}_e\frac{\partial}{\partial \tau_e^l}\Big(\frac{\partial u_N^{n+1}}{\partial \boldsymbol{n}_e}\Big) + \sum_{m=1}^{d-1}\alpha\cdot\tau_e^m\frac{\partial}{\partial\tau_e^m}\Big(\frac{\partial u_N^{n+1}}{\partial \tau_e^m}\Big),\quad 1\le l\le d-1.\end{aligned}$$

By direct calculations we get that on each edge/face e of $K\in\mathcal{Q}_h$, taking $v_N = \alpha\cdot\nabla u_N^{n+1}$,

$$\begin{aligned}\frac{\partial v_N}{\partial \boldsymbol{n}_e} &= \frac{\partial u_N^{n+1}}{\partial \boldsymbol{n}_e} + \alpha\cdot\nabla\frac{\partial u_N^{n+1}}{\partial \boldsymbol{n}_e}\\ &= \frac{\partial u_N^{n+1}}{\partial \boldsymbol{n}_e} + \alpha\cdot\boldsymbol{n}_e\frac{\partial^2 u_N^{n+1}}{\partial \boldsymbol{n}_e^2} + \sum_{m=1}^{d-1}\alpha\cdot\tau_e^m\frac{\partial}{\partial\tau_e^m}\Big(\frac{\partial^2 u_N^{n+1}}{\partial \boldsymbol{n}_e^2}\Big),\\ \frac{\partial^2 v_N}{\partial \boldsymbol{n}_e^2} &= 2\frac{\partial^2 u_N^{n+1}}{\partial \boldsymbol{n}_e^2} + \alpha\cdot\boldsymbol{n}_e\frac{\partial^3 u_N^{n+1}}{\partial \boldsymbol{n}_e^3} + \sum_{m=1}^{d-1}\alpha\cdot\tau_e^m\frac{\partial}{\partial\tau_e^m}\Big(\frac{\partial^2 u_N^{n+1}}{\partial \boldsymbol{n}_e^2}\Big).\end{aligned}$$

By induction, it follows that

$$\frac{\partial^j v_N}{\partial \boldsymbol{n}_e^j} = j\frac{\partial^j u_N^{n+1}}{\partial \boldsymbol{n}_e^j} + \alpha\cdot\boldsymbol{n}_e\frac{\partial^{j+1} u_N^{n+1}}{\partial \boldsymbol{n}_e^{j+1}} + \sum_{m=1}^{d-1}\alpha\cdot\tau_e^m\frac{\partial}{\partial\tau_e^m}\Big(\frac{\partial^j u_N^{n+1}}{\partial \boldsymbol{n}_e^j}\Big),\quad 1\le j\le N-1. \tag{A.10}$$

Specially, if $j=N$, then we have

$$\frac{\partial^N v_N}{\partial \boldsymbol{n}_e^N} = N\frac{\partial^N u_N^{n+1}}{\partial \boldsymbol{n}_e^N}. \tag{A.11}$$

For $j=1,2,\cdots,q-1$, in view of (A.10), we get

$$\begin{aligned}&-2\mathrm{Im}\Big(J_j(u_N^{n+1},v_N)\Big)\\ =&-2\mathrm{Im}\sum_{e\in\mathcal{E}_h^I}\gamma_{j,e}\Big(\frac{|e|}{N}\Big)^{2j-1}\Big(\alpha\cdot\boldsymbol{n}_e\Big\langle\Big[\frac{\partial^j u_N^{n+1}}{\partial \boldsymbol{n}_e^j}\Big],\Big[\frac{\partial^{j+1} u_N^{n+1}}{\partial \boldsymbol{n}_e^{j+1}}\Big]\Big\rangle_e\\ &+\sum_{m=1}^{d-1}\alpha\cdot\tau_e^m\Big\langle\Big[\frac{\partial^j u_N^{n+1}}{\partial \boldsymbol{n}_e^j}\Big],\Big[\frac{\partial}{\partial\tau_e^m}\Big(\frac{\partial^j u_N^{n+1}}{\partial \boldsymbol{n}_e^j}\Big)\Big]\Big\rangle_e\Big)\\ \lesssim&\sum_{e\in\mathcal{E}_h^I}\gamma_{j,e}\Big(\frac{|e|}{N}\Big)^{2j-1}\Big\|\Big[\frac{\partial^j u_N^{n+1}}{\partial \boldsymbol{n}_e^j}\Big]\Big\|_{L^2(e)}\Big(\Big\|\Big[\frac{\partial^{j+1} u_N^{n+1}}{\partial \boldsymbol{n}_e^{j+1}}\Big]\Big\|_{L^2(e)}+\frac{N^2}{|e|}\Big\|\Big[\frac{\partial^j u_N^{n+1}}{\partial \boldsymbol{n}_e^j}\Big]\Big\|_{L^2(e)}\Big)\\ \lesssim&\sum_{e\in\mathcal{E}_h^I}\frac{N}{|e|}\sqrt{\frac{\gamma_{j,e}}{\gamma_{j+1,e}}}\Big(\gamma_{j,e}\Big(\frac{|e|}{N}\Big)^{2j-1}\Big\|\Big[\frac{\partial^j u_N^{n+1}}{\partial \boldsymbol{n}_e^j}\Big]\Big\|_{L^2(e)}^2\\ &+\gamma_{j+1,e}\Big(\frac{|e|}{N}\Big)^{2j+1}\Big\|\Big[\frac{\partial^{j+1} u_N^{n+1}}{\partial \boldsymbol{n}_e^{j+1}}\Big]\Big\|_{L^2(e)}^2\Big)+\sum_{e\in\mathcal{E}_h^I}\frac{N^2}{|e|}\gamma_{j,e}\Big(\frac{|e|}{N}\Big)^{2j-1}\Big\|\Big[\frac{\partial^j u_N^{n+1}}{\partial \boldsymbol{n}_e^j}\Big]\Big\|_{L^2(e)}^2.\end{aligned} \tag{A.12}$$

If $q<N$, then from the inverse inequality it follows

$$\begin{aligned}-2\mathrm{Im}\Big(J_q(u_N^{n+1},v_N)\Big) =& -2\mathrm{Im}\Big(\sum_{e\in\mathcal{E}_h^I}\gamma_{q,e}\Big(\frac{|e|}{N}\Big)^{2q-1}\Big\langle\Big[\frac{\partial^q u_N^{n+1}}{\partial \boldsymbol{n}_e^q}\Big],\Big[\frac{\partial^q v_N}{\partial \boldsymbol{n}_e^q}\Big]\Big\rangle_e\Big)\\ \le&\frac{1}{8}\,|u_N^{n+1}|_{1,\mathcal{Q}_h}^2 + C\sum_{e\in\mathcal{E}_h^I}\frac{\gamma_{q,e}N^{2q+3}}{|e|^2}\gamma_{q,e}\Big(\frac{|e|}{N}\Big)^{2q-1}\Big\|\Big[\frac{\partial^q u_N^{n+1}}{\partial \boldsymbol{n}_e^q}\Big]\Big\|_{L^2(e)}^2.\end{aligned}$$

If $q \geq N$, (A.11) and the definition of $J_q(\cdot,\cdot)$ immediately imply that $2\mathrm{Im}\big(J_q(u_N^{n+1}, v_N)\big) = 0$. The term $-2\mathrm{Im}\big(J_0(u_N^{n+1}, v_N)\big)$ can be treated as

$$
\begin{aligned}
-2\mathrm{Im}\big(J_0(u_N^{n+1}, v_N)\big) &= -2\mathrm{Im} \sum_{e\in\mathcal{E}_h^{IB}} \frac{\gamma_{0,e}N}{|e|}\Big\langle [u_N^{n+1}], [\alpha\cdot \boldsymbol{n}_e \frac{\partial u_N^{n+1}}{\partial \boldsymbol{n}_e} + \sum_{j=1}^{d-1} \alpha\cdot\tau_e^j \frac{\partial u_N^{n+1}}{\partial \tau_e^j}]\Big\rangle_e \\
&\leq -2\mathrm{Im} \sum_{e\in\mathcal{E}_h^B} \frac{\gamma_{0,e}N}{|e|}\Big\langle \alpha\cdot\boldsymbol{n}_e u_N^{n+1}, \frac{\partial u_N^{n+1}}{\partial \boldsymbol{n}_e}\Big\rangle_e + C\sum_{e\in\mathcal{E}_h^{IB}} \frac{N^2}{|e|}\frac{\gamma_{0,e}N}{|e|}\left\|[u_N^{n+1}]\right\|_{L^2(e)}^2 \\
&\quad + C\sum_{e\in\mathcal{E}_h^I} \frac{N}{|e|}\sqrt{\frac{\gamma_{0,e}}{\gamma_{1,e}}}\Big(\frac{\gamma_{0,e}N}{|e|}\left\|[u_N^{n+1}]\right\|_{L^2(e)}^2 + \frac{\gamma_{1,e}|e|}{N}\Big\|\Big[\frac{\partial u_N^{n+1}}{\partial \boldsymbol{n}_e}\Big]\Big\|_{L^2(e)}^2\Big).
\end{aligned}
$$

We also need the following estimate

$$
\begin{aligned}
&\sum_{e\in\mathcal{E}_h^B}\Big(\langle\alpha\cdot\boldsymbol{n}_e, |\nabla u_N^{n+1}|^2\rangle_e + k^2\langle\alpha\cdot\boldsymbol{n}_e, |u_N^{n+1}|^2\rangle_e - 2\frac{\gamma_{0,e}N}{|e|}\mathrm{Im}\Big\langle\alpha\cdot\boldsymbol{n}_e u_N^{n+1}, \frac{\partial u_N^{n+1}}{\partial \boldsymbol{n}_e}\Big\rangle_e\Big) \\
&\leq -C_B\sum_{e\in\mathcal{E}_h^B}\Big(k^2\left\|u_N^{n+1}\right\|_{L^2(e)}^2 + \frac{1}{2}\left\|\nabla u_N^{n+1}\right\|_{L^2(e)}^2\Big) + C\sum_{e\in\mathcal{E}_h^B}\Big(\frac{\gamma_{0,e}N}{|e|}\Big)^2\left\|u_N^{n+1}\right\|_{L^2(e)}^2,
\end{aligned}
\tag{A.13}
$$

where we have used the inverse inequality and the assumption that D is a star-shape domain.

Step 3: Substituting (A.8)-(A.13) into (A.7), and using (A.13) we obtain

$$
\begin{aligned}
&\frac{15}{8}k^2\left\|u_N^{n+1}\right\|_{L^2(\Omega)}^2 \\
&\leq \frac{1}{8}\mathrm{Re}\Big((f, u_N^n) + \langle\delta_k u_N^n, u_N^{n+1}\rangle_{\Gamma_R}\Big) - \frac{k}{8}\mathrm{Re}(D_k)\langle u_N^{n+1}, u_N^{n+1}\rangle_{\Gamma_R} + CM(f, \delta_k u_N^n)^2 \\
&\quad + \frac{5}{8}\left|u_N^{n+1}\right|_{1,\mathcal{Q}_h}^2 + \frac{k^2}{8}\|u_N^{n+1}\|_{L^2(\Omega)}^2 - \frac{C_{\Omega_R}}{4}\sum_{e\in\mathcal{E}_h^R}\left\|\nabla u_N^{n+1}\right\|_{L^2(e)}^2 + Ck^2\left\|u_N^{n+1}\right\|_{L^2(\Gamma_R)}^2 \\
&\quad - \frac{1}{8}\sum_{K\in\mathcal{Q}_h}\left\|\nabla u_N^{n+1}\right\|_{L^2(k)}^2 - 2\sum_{e\in\mathcal{E}_h^{IB}}\mathrm{Re}\Big\langle\Big\{\frac{\partial u_N^{n+1}}{\partial \boldsymbol{n}_e}\Big\}, [u_N^{n+1}]\Big\rangle_e \\
&\quad + C\sum_{e\in\mathcal{E}_h^{IB}}\Big(\frac{N^5}{\gamma_{0,e}|e|^2} + \frac{N}{\gamma_{0,e}} + \frac{N^2}{|e|}\Big)\frac{\gamma_{0,e}N}{|e|}\left\|[u_N^{n+1}]\right\|_{L^2(e)}^2 \\
&\quad + C\sum_{j=1}^{q-1}\sum_{e\in\mathcal{E}_h^I}\Big(\frac{N}{|e|}\Big(\sqrt{\frac{\gamma_{j,e}}{\gamma_{j+1,e}}} + N\Big)\gamma_{j,e}\Big(\frac{|e|}{N}\Big)^{2j-1}\Big\|\Big[\frac{\partial u_N^{n+1}}{\partial \boldsymbol{n}_e}\Big]\Big\|_{L^2(e)}^2 \\
&\qquad\qquad + \frac{N}{|e|}\sqrt{\frac{\gamma_{j,e}}{\gamma_{j+1,e}}}\gamma_{j+1,e}\Big(\frac{|e|}{N}\Big)^{2j+1}\Big\|\Big[\frac{\partial^{j+1}u_N^{n+1}}{\partial \boldsymbol{n}_e^{j+1}}\Big]\Big\|_{L^2(e)}^2\Big) \\
&\quad + C\sum_{e\in\mathcal{E}_h^I}\frac{\gamma_{q,e}N^{2q+3}}{|e|^2}\gamma_{q,e}\Big(\frac{|e|}{N}\Big)^{2q-1}\Big\|\Big[\frac{\partial^q u_N^{n+1}}{\partial \boldsymbol{n}_e^q}\Big]\Big\|_{L^2(e)}^2 + C\sum_{e\in\mathcal{E}_h^I}\frac{N}{|e|}\sqrt{\frac{\gamma_{0,e}}{|e|}}\frac{\gamma_{0,e}N}{|e|}\left\|[u_N^{n+1}]\right\|_{L^2(e)}^2 \\
&\quad + C\sum_{e\in\mathcal{E}_h^I}\frac{N}{|e|}\sqrt{\frac{\gamma_{0,e}}{\gamma_{1,e}}}\frac{\gamma_{1,e}|e|}{N}\Big\|\Big[\frac{\partial u_N^{n+1}}{\partial \boldsymbol{n}_e}\Big]\Big\|_{L^2(e)}^2 - C_B\sum_{e\in\mathcal{E}_h^B}\Big(k^2\left\|u_N^{n+1}\right\|_{L^2(e)}^2 \\
&\qquad\qquad + \frac{1}{2}\left\|\nabla u_N^{n+1}\right\|_{L^2(e)}^2\Big) + C\sum_{e\in\mathcal{E}_h^B}\frac{\gamma_{0,e}N}{|e|}\frac{\gamma_{0,e}N}{|e|}\left\|[u_N^{n+1}]\right\|_{L^2(e)}^2.
\end{aligned}
$$

Therefore, it follows from Lemma 3.1, the bound (3.16) of the real part of $a_N(u_N^{n+1}, u_N^{n+1})$, and definition of C_{stab} that

$$\begin{aligned}&\frac{15}{8}k^2\left\|u_N^{n+1}\right\|^2_{L^2(\Omega)} + \frac{1}{2}\left|u_N^{n+1}\right|^2_{1,\mathcal{Q}_h} + \frac{C_{\Omega_R}}{4}\sum_{e\in\mathcal{E}_h^R}\left\|\nabla u_N^{n+1}\right\|^2_{L^2(e)}\\&\quad + C_B\sum_{e\in\mathcal{E}_h^B}\Big(k^2\left\|u_N^{n+1}\right\|^2_{L^2(e)} + \frac{1}{2}\left\|\nabla u_N^{n+1}\right\|^2_{L^2(e)}\Big)\\&\le CM^2(f,\delta_k u_N^n) + \frac{9k^2}{8}\left\|u_N^{n+1}\right\|^2_{L^2(\Omega)} - \frac{9}{8}k\mathrm{Re}(D_k)\langle u_N^{n+1}, u_N^{n+1}\rangle_{\Gamma_R}\\&\quad + Ck^2C_{stab}\left|(f,u_N^{n+1}) + \langle\delta_k u_N^n, u_N^{n+1}\rangle_{\Gamma_R}\right|,\end{aligned}\tag{A.14}$$

where we derive the inequality by also using a consequence of (3.17):

$$Ck^2\left\|u_N^{n+1}\right\|^2_{L^2(\Gamma_R)} \le C\frac{k}{|\mathrm{Im}(D_k)|}\left|(f,u_N^{n+1}) + \langle\delta_k u_N^n, u_N^{n+1}\rangle_{\Gamma_R}\right|.$$

From Lemma 3.1, it follows

$$Ck^2C_{stab}\left|(f,u_N^{n+1}) + \langle\delta_k u_N^n, u_N^{n+1}\rangle_{\Gamma_R}\right| \le Ck^2C_{stab}^2M^2(f,\delta_k u_N^n) + \frac{k^2}{8}\left\|u_N^{n+1}\right\|^2_{L^2(\Omega)},$$

then (A.14) can be written as

$$\begin{aligned}&\frac{5}{8}k^2\left\|u_N^{n+1}\right\|^2_{L^2(\Omega)} + \frac{1}{2}\left|u_N^{n+1}\right|^2_{1,\mathcal{Q}_h} + \frac{C_{\Omega_R}}{4}\sum_{e\in\mathcal{E}_h^R}\left\|\nabla u_N^{n+1}\right\|^2_{L^2(e)}\\&+\frac{9}{8}k\mathrm{Re}(D_k)\sum_{e\in\mathcal{E}_h^R}\left\|u_N^{n+1}\right\|^2_{L^2(e)} + C_B\sum_{e\in\mathcal{E}_h^B}\Big(k^2\left\|u_N^{n+1}\right\|^2_{L^2(e)} + \frac{1}{2}\left\|\nabla u_N^{n+1}\right\|^2_{L^2(e)}\Big)\\&\le Ck^2C_{stab}^2M^2(f,\delta_k u_N^n),\end{aligned}$$

which completes the proof. □

Acknowledgments. The work of the first author was partially supported by the National Natural Science Foundation of China (11026065 and 11101196). This work was largely done when this author worked as a Research Fellow in Nanyang Technological University. The work of the second author was supported by the National Natural Science Foundation of China (11201166). The work of the third author was supported by Singapore MOE Tier 1 Grant (2013-2016), and Singapore A*STAR-SERC-PSF Grant 122-PSF-0007.

References

[1] D.N. Arnold, An interior penalty finite element method with discontinuous elements, *SIAM J. Numer. Anal.*, **19**:4 (1982), 742-760.

[2] D.N. Arnold, F. Brezzi, B. Cockburn, and L.D. Marini, Unified analysis of discontinuous Galerkin methods for elliptic problems, *SIAM J. Numer. Anal.*, **39**:5 (2002), 1749-1779.

[3] A.K. Aziz and A. Werschulz, On the numerical solution of Helmholtz's equation by the finite element method, *SIAM J. Numer. Anal.*, **17**:5 (1980), 681-686.

[4] I. Babuška, F. Ihlenburg, E.T. Paik, and S.A. Sauter, A generalized finite element method for solving the Helmholtz equation in two dimensions with minimal pollution, *Comp. Meth. Appl. Mech. Eng.*, **128**:3-4 (1995), 325-359.

[5] G. Bao, Finite element approximation of time harmonic waves in periodic structures, *SIAM J. Numer. Anal.*, **32**:4 (1995), 1155-1169.

[6] J.P. Berenger, A perfectly matched layer for the absorption of electromagnetic waves, *J. Comput. Phys.*, **114**:2 (1994), 185-200.

[7] S.N. Chandler-Wilde and P. Monk, Wave-number-explicit bounds in time-harmonic scattering, *SIAM J. Math. Anal*, **39**:5 (2008), 1428-1455.

[8] P.G. Ciarlet, The Finite Element Method for Elliptic Problems, North-Holland, 1978.

[9] R.D. Ciskowski and C.A. Brebbia, Boundary Element Methods in Acoutics, Kluwer Academic Publishers, 1991.

[10] B. Cockburn, G.E. Karniadakis, and C.W. Shu, Discontinuous Galerkin methods: Theory, Computation and Applications, volume 11 of Lecture Notes in Computational Science and Engineering, Springer Verlag, Berlin, 2000.

[11] P. Cummings, X. Feng, and S. Lenhart, Sharp regularity coefficient estimates for complex-valued acoustic and elastic Helmholtz equations, *Math. Models Methods Appl. Sci.*, **16**:1 (2006), 139-160.

[12] L. Demkowicz and F. Ihlenburg, Analysis of a coupled finite-infinite element method for exterior Helmholtz problems, *Numer. Math.*, **88**:1 (2001), 43-73.

[13] J. Douglas, J.E. Santos, D. Sheen, and L.S. Bennethum, Frequency domain treatment of one-dimensional scalar waves, *Math. Models Methods Appl. Sci*, **3** (1993), 171-194.

[14] Q.R. Fang, D.P. Nicholls, and J. Shen, A stable, high-order method for three-dimensional, bounded-obstacle, acoustic scattering, *J. Comput. Phys.*, **224**:2 (2007), 1145-1169.

[15] X. Feng and H. Wu, Discontinuous Galerkin methods for the Helmholtz equation with large wave number, *SIAM J. Numer. Anal.*, **47** (2009), 2872-2896.

[16] X. Feng and H. Wu, *hp*-discontinuous Galerkin methods for the Helmholtz equation with large wave number, *Math. Comp.*, **80**:276 (2011), 1997-2024.

[17] K. Gerdes and L. Demkowicz, Solution of 3D-Laplace and Helmholtz equations in exterior domains using $hp-$ infinite elements, *Comput. Methods Appl. Mech. Engrg.*, **137** (1996), 239-273.

[18] I. Harari and T.J.R. Hughes, Analysis of continuous formulations underlying the computation of time-harmonic acoustics in exterior domains, *Comput. Methods Appl. Mech. Engrg.*, **97**:1 (1992), 103-124.

[19] U. Hetmaniuk, Stability estimates for a class of Helmholtz problems, *Commun. Math. Sci.*, **5**:3 (2007), 665-678.

[20] I. Babuška and S.A. Sauter, Is the pollution effect of the FEM avoidable for the Helmholtz equation considering high wave numbers?, *SIAM Review*, **42**:3 (2000), 451-484.

[21] F. Ihlenburg, Finite Element Analysis of Acoustic Scattering, Volume 132 of Applied Mathematical Sciences, Springer Verlag, New York, 1998.

[22] F. Ihlenburg and I. Babuška, Finite element solution of the Helmholtz equation with high wave number. II. The *h-p* version of the FEM, *SIAM J. Numer. Anal.*, **34**:1 (1997), 315-358.

[23] J.B. Keller and D. Givoli, Exact non-reflecting boundary conditions, *J. Comput. Phys.*, **82** (1989), 172-192.

[24] J.M. Melenk, On Generalized Finite Element Methods, PhD thesis, University of Maryland, College Park, 1995.

[25] J.M. Melenk and S. Sauter, Convergence analysis for finite element discretizations of the Helmholtz equation with Dirichlet-to-Neumann boundary conditions, *Math. Comp.*, **79** (2010), 1871-1914.

[26] P.M. Morse and H. Feshback, Methods of Theoretical Physics, McGraw-Hill, New York, 1953.

[27] J.C. Nédélec, Acoustic and Electromagnetic Equations: Integral Representations for Harmonic Problems, Springer Verlag, 2001.

[28] D. Nicholls and F. Reitich, Analytic continuation of Dirichlet-Neumann operators, *Numer. Math.*, **94**:1 (2003), 107-146.

[29] D. Nicholls and J. Shen, A stable, high–order method for two–dimensional bounded–obstacle scattering, *SIAM J. Sci. Comput.*, **28** (2006), 1398-1419.

[30] D.P. Nicholls and J. Shen, A rigorous numerical analysis of the transformed field expansion method, *SIAM J. Numer. Anal.*, **47**:4 (2009), 2708-2734.

[31] B. Rivière, Discontinuous Galerkin Methods for Solving Elliptic and Parabolic Equations: Theory and Implementation, SIAM, 2008.

[32] A.H. Schatz, An observation concerning Ritz-Galerkin methods with indefinite bilinear forms, *Math. Comp.*, **28**:128 (1974), 959-962.

[33] J. Shen, T. Tang, and L.L. Wang, Spectral Methods: Algorithms, Analysis and Applications, volume 41 of Springer Series in Computational Mathematics, Springer-Verlag, Berlin, Heidelberg, 2011.

[34] J. Shen and L.L. Wang, Spectral approximation of the Helmholtz equation with high wave numbers, *SIAM J. Numer. Anal.*, **43**:2 (2005), 623-644.

[35] J. Shen and L.L. Wang, Analysis of a spectral-Galerkin approximation to the Helmholtz equation exterior domains, *SIAM J. Numer. Anal.*, **45**:5 (2007), 1954-1978.

[36] G.N. Watson, A Treatise on the Theory of Bessel Functions, Cambridge University Press, 1966.